

GRAS SAF




GRAS Meteorology SAF

- 1. GRAS SAF Visiting Scientist Activity No. 8**
High-resolution radiosondes for GRAS Level 2 validation
- 2. Ref: SAF/GRAS/DMI/REP/VS8/001**
- 3. 18 April 2008 , Version 1.0 ,**

**Mark Smees and John Nash,
Observation Research and Development, Met Office.**

Prepared by:
Danish Meteorological Institute (DMI)
European Centre for Medium-Range Weather Forecasts (ECMWF)
Institut d'Estudis Espacials de Catalunya (IEEC)
Met Office (MetO)


Ref: SAF/GRAS/DMI/REP/VS8/001 Issue: Version 1.0 Date: 23 May 2008 Document: VS8-report_18-04-08_v10.doc	GRAS Meteorology SAF Document	EUMETSAT DMI ECMWF IEEC Met Office	 www.grassaf.org
---	----------------------------------	--	--

DOCUMENT SIGNATURE TABLE

	Name	Function	Date	Signature
Prepared by:	DMI, Met Office, IEEC, ECMWF	GRAS SAF Project Team	29/10/07	
Approved by:	Kent B. Lauritsen	GRAS SAF Project Manager	29/10/07	

DOCUMENTATION CHANGE RECORD

Issue / Revision	Date	By	Description
1.0	18/04/08	Met Office	Edited Version

Ref: SAF/GRAS/DMI/REP/VS8/001 Issue: Version 1.0 Date: 23 May 2008 Document: VS8-report_18-04-08_v10.doc	GRAS Meteorology SAF Document	EUMETSAT DMI ECMWF IEEC Met Office	 www.grassaf.org
---	----------------------------------	--	--

High resolution radiosondes for GRAS Level 2 validation- Part I

J. Nash and M. Smees

Upper Air Team,
Observation Development
Met Office
Fitzroy Road,
Exeter EX1 3PB
Tel +44-1392-885649: e-mail: john.nash@metoffice.gov.uk

GRAS SAF Visiting Scientist, October 2007

1. Introduction

The purpose of this study was to use data from the German CHAMP (CHALLENGING Minisatellite Payload, Reigber et al. [2005] , to examine whether high resolution radiosonde data (from Part B and D of the TEMP message) would provide a better fit to the CHAMP measurements than the radiosonde standard pressure level data (from Part A and C of the TEMP message) used in earlier studies.

The results from this study would then be used to recommend methods to validate GRAS data in addition to the comparison of GRAS output with Numerical Weather Prediction [NWP] fields.

It was thought that the radio occultation measurements had inherently higher vertical resolution in temperature measurements than could be checked by comparing with the limited number of NWP model levels in the stratosphere or the standard pressure levels in the radiosonde TEMP messages. This type of study had been performed by Wickert [2004] for data sampled between 2001 and 2004. Wickert found that the standard deviation between the CHAMP and Radiosonde temperature observations at 100 hPa was typically about 1.7 to 1.9 K in Europe , the former Soviet Union and the USA. At 10 hPa the equivalent standard deviation was in the range 3 to 3.5 K for the better radiosonde measurements.

2. Radio occultation measurements

Technical descriptions of atmospheric sounding by GPS occultation are contained amongst others in Kursinski et al [1997] and Hajj, et al [2002]. In Hajj, et al, GPS/MET comparisons with ECMWF NWP fields in the northern hemisphere were cited as having a standard deviation of 1.5 K. For the purpose of this study it has to be recognised that the reported atmospheric profiles are the result of bending in the atmosphere not purely at the tangent but over a significant distance in the horizontal [70 per cent of the bending occurs over a path length of about 470 km, with the tangent point drifting up to a 100km in the horizontal during an individual profile measurement]. So in attempting to validate radio occultation measurements it would be wise to choose those circumstances when there were no large temperature gradients

in the horizontal in the vicinity of the radiosondes used and to ensure that the radiosonde profiles are as representative as possible of a relatively large volume of the atmosphere.

In recent examination of the use of the GPS radio occultation measurements by Healy et al (2006), some of the limitations in the forward models of the bending were examined including some of the assumptions that are necessary in order to solve for the bending angles/changes in refractivity in the vertical. This study suggests that errors may exist in the heights assigned to the profiles in some conditions, with the problem probably more significant in the lower troposphere.

3. Radiosonde measurements.

3.1 Sensor errors

The majority of radiosondes used in this study were Vaisala RS80 types. Most RS80 radiosondes transmitted data at 403 MHz, but some transmitted data to the ground station at 1680MHz. Various types of wind measurement were used with these radiosondes, hence the different types. With the GPS radiosondes the position of the antenna for receiving GPS signals on the radiosonde could affect the shading of the radiosonde temperature sensor from the sun. The shading seemed to vary from flight to flight, because of the complex motions of the radiosonde during an ascent. Random errors in daytime temperature measurements were larger than in night-time measurements with these radiosondes.

The quality of the temperature measurements of the RS80 radiosondes have been studied in some detail in the early WMO Radiosonde Comparison Tests, Nash and Schmidlin [1987], Ivanov, et al [1991], Yagi et al [1996].

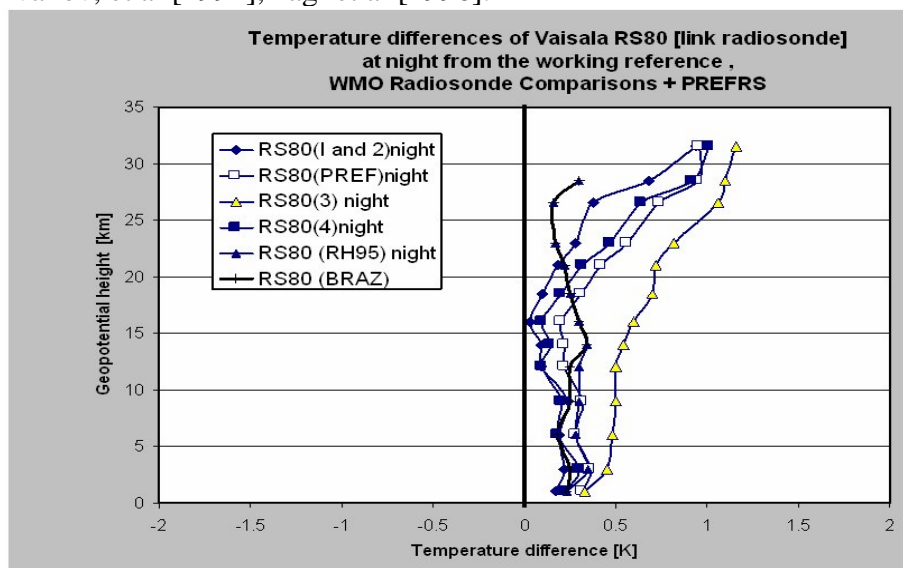


Fig.3.1.1 Temperature differences of Vaisala RS80 radiosonde at night relative to working references from the early WMO Radiosonde Comparison tests and the Potential Reference Radiosonde [PREFRS] test performed in the UK in 1992.

The variation in performance of the RS80 temperature measurements at night was estimated from 4 WMO tests performed in 1984, 1985, 1989 and 1993 and from a special test of reference quality radiosondes [PREFRS] performed in 1992, Nash [1994]. At night differences between the four WMO tests were thought to be small and of the order of ± 0.3 K at worst, except for one exceptional batch of radiosondes when there was problems in the manufacturers calibration facility, see Fig.3.1.1. These calibration problems have not recurred in recent years. The positive bias in night-time temperature at upper levels is not present in recent measurements, because it was the result of an error in radiation corrections at night which was introduced in early versions of processing software and was not used in recent years.

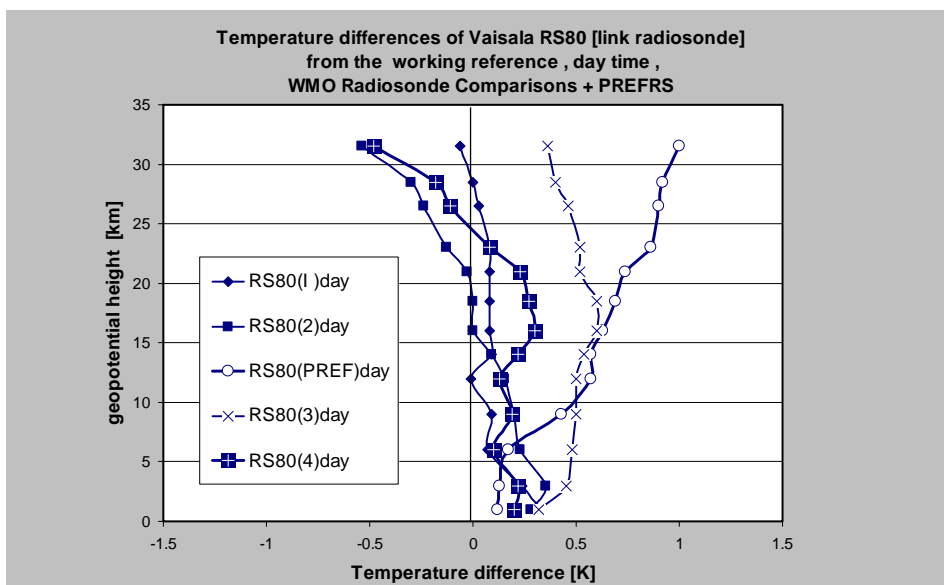



Fig.3.1.2 Temperature differences of Vaisala RS80 radiosonde in the day relative to working references from the early WMO Radiosonde Comparison tests and the Potential Reference Radiosonde [PREFRS] test performed in the UK in 1992. Multithermistor radiosondes used as reference in 4 and PREFRS.

In the daytime there was a wider spread in estimated temperature performance between the different tests, see Fig.3.1.2. Here, the measurements in the three later tests were compared against the results from multithermistor radiosondes, Schmidlin [1992]. The multithermistor technique corrects for the radiative heating of the sensors by comparing the measurements of sensors with three different coatings of known optical properties. The larger spread in the RS80 temperature measurements [which are an average from at least 15 comparison flights per test] is because the temperature sensors are heated by the sun, but the average heating changes according to the prevalent surface and cloud conditions in the test . The corrections applied by the software are only valid for certain surface and cloud albedo. Over the sea [low albedo] in relatively cloud free conditions , as experienced in WMO tests 2 and 4, the daytime corrections were too big at high altitudes. Over thick cirrus cloud in PREFRS the heating corrections were too small.

Ref: SAF/GRAS/DMI/REP/VS8/001 Issue: Version 1.0 Date: 23 May 2008 Document: VS8-report_18-04-08_v10.doc	GRAS Meteorology SAF Document	EUMETSAT DMI ECMWF IEEC Met Office	 www.grassaf.org
---	----------------------------------	--	--

On the basis of these test results , the radiosonde temperature at night for a set of about 15 radiosondes could reasonably be expected to be reproducible to about $\pm 0.3\text{K}$ and in the day-time up to about 25 km to about $\pm 0.4\text{ K}$.

Sites where the radiosonde practices are bad or not typical of that measured in the WMO Radiosonde Comparison can be identified from the quality monitoring of geopotential heights reported by the radiosonde stations.. The standard deviation of 100 geopotential height against the background forecast should be lower than 25m for a good quality radiosonde site and systematic bias at 100 hPa should be within about $\pm 25\text{ m}$ of the background forecast.

See Instruments and Methods of Observation Programme Monitoring Reports, Upper-air monitoring statistics for 2005

<http://www.wmo.ch/pages/prog/www/IMOP/monitoring.html>

At some times of the year the measurements by the Vaisala RS80 in the USA may have large systematic errors which are not typical of the RS80 in the rest of the world. These results from a fault in the radiation correction applied to the temperature measurements by the US ground system software. The stations with bad measurements can be avoided by checking for large systematic bias relative to the background forecasts, mostly occurring at pressures lower than 100 hPa.

Height assignment errors in the reported temperatures can be assumed to be relatively small with the RS80 radiosonde. Systematic errors should be less than 1 hPa error in pressure [less than 65 m error in geopotential height at 100 hPa], as long as the radiosonde operators prepare the radiosonde correctly. Stations where the observing practices are poor, e.g. faulty surface pressure measurements can be avoided by checking the quality monitoring results.

For the future, most of the RS80 radiosondes are being replaced by the RS92 radiosonde which has a much faster temperature sensor . This leads to a much smaller average heating error, so variation in daytime temperature errors should be much less than with the RS80. Similarly, the RS92 pressure sensor is more accurate than the RS80 pressure sensor and also the GPS tracking can be used to measure height in a very reproducible fashion, with random errors less than 10m up to 35 km, see Nash et al [2006]. It is hoped that these radiosondes might allow the accuracy of temperature measurements made by modern radiosondes to be within $\pm 0.2\text{K}$ in both day and night measurements, but the measurements to identify the real limits of this radiosonde type are only just starting. The Japanese radiosonde temperature measurements will be similar to those of the RS80. The American VIZ/Sippican radiosonde temperatures will be slightly poorer and accuracy would probably be about $\pm 0.5\text{K}$.

3.2 Limitations of TEMP code reports

Operational radiosonde messages are mainly communicated over the Global Telecommunication System in TEMP code. This code was designed for the days when radiosonde data were derived manually by the radiosonde operators, so the values at standard pressure levels are reported in Parts A and C of the message, and then a set of significant levels for temperature

and humidity [in terms of dew point depression] and also for winds are reported in Parts B and D. If a linear interpolation against height were performed between the significant levels , the WMO rules suggested that the interpolated temperature should not have errors larger than 1 K from the actual measurements in the troposphere and 2 K in the stratosphere , relative humidity should not be in error by more than 15 per cent in the troposphere, and winds should not have errors larger than 5 ms^{-1} and wind direction greater than 10° . These fitting limits are too crude to retain the full accuracy of the modern radiosonde sensor measurements, and in some countries the fitting limits have been halved to improved the reporting accuracy.

The fitting limits mean that probably at best , the regenerated TEMP message received by the users would be likely to have random temperature errors of at least 0.3K in the troposphere and 0.6 K in the stratosphere introduced by the coding procedures in addition to the random errors associated with the actual sensor measurements.

This limitation can be overcome by obtaining the full archived data from the radiosonde station, but in this study this has not been done since it was clear that coding errors were not the main limiting factor in the standard deviations of the comparisons.

In future , it is intended that the full radiosonde measurements will be supplied to users by implementation of a suitable BUFR code to replace TEMP code , and this is expected to be achieved within a few years

3.3 Representativeness errors in radiosonde temperature and relative humidity

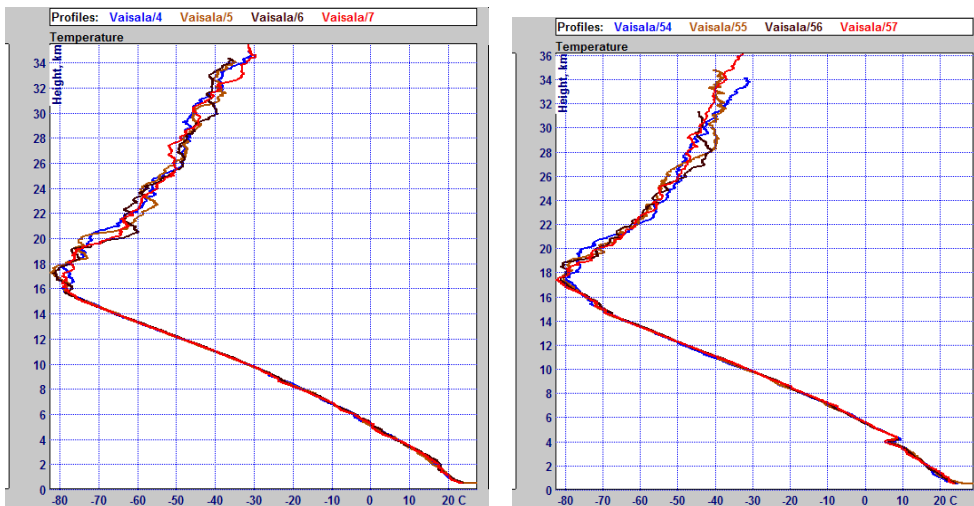


Fig. 3.3.1 Comparison of four radiosonde temperature measurements within 14 hours on two different days, demonstrating the influence of small scale atmospheric motions in the stratosphere, WMO High Quality Radiosonde test, Mauritius, 2005.

In Part II of this report, most collocated observations have been obtained in the tropics and Fig. 3.3.1 shows an example of the limitations of the radiosonde sample in the tropics. In the upper troposphere there is little variation in temperature with time, but in the stratosphere the measurements vary rapidly with time, because of the small scale temperature fluctuations associated with various types of gravity waves. So in this study, radiosonde measurements have been grouped together to average out the effects of the transient gravity waves. However, on looking at the vertical structure in the CHAMP temperature profiles supplied for this evaluation by DMI, variations with vertical wavelengths of about 2 km, typical of the slow moving gravity waves with large horizontal wavelengths do not seem to be evident. This is because the CHAMP profiles supplied were the result of a 1-dVAR retrieval against ECMWF background fields/ model data for temperature and these model fields do not seem to retain the gravity wave structures.

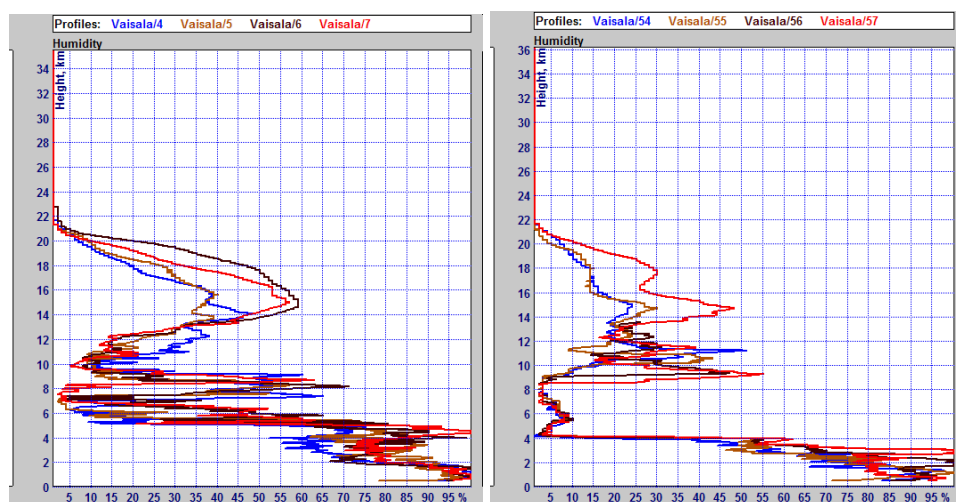


Fig.3.3.2 Comparison of four radiosonde relative humidity measurements within 14 hours, demonstrating the large variability of relative humidity in some layers in the troposphere, and the small variability in others over relatively short periods, WMO High Quality Radiosonde test, Mauritius, 2005.

Relative humidity measurements vary rapidly in space and time, see Fig. 3.3.2, even when the basic vertical structure is not changing that rapidly. Unlike temperature it is unwise to interpolate over relatively large distances, so precise validation of relative humidity would require a special observing network with radiosondes closer together than is usually found in the radiosondes of the Global Observing system at the moment.

A quantitative estimate of the temperature variability sampled by the radiosondes in the tropics is shown in Fig. 3.3.3 where the standard deviations of 4 measurements performed in less than a day against the average value for the day is shown for six different days as sampled in the rainy season in Mauritius in 2005. So, in most of the troposphere the radiosonde measurements probably have a representativeness error of about 0.3K, whereas in the stratosphere the individual measurements probably have a representativeness error of about 1 K. Similar results were obtained from a slightly smaller data set obtained at Dar-es-Salaam in Tanzania in 2004, see Fig.3.3.4. In this case the surface temperatures varied more during the day so there was more variability near the surface than in Mauritius.

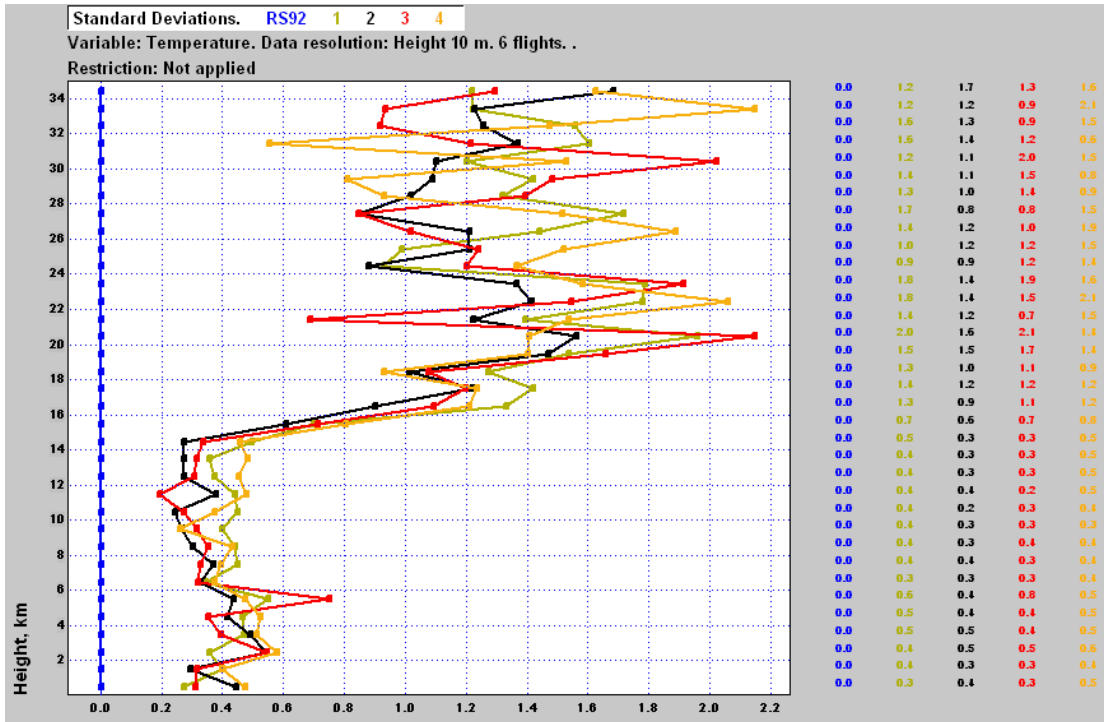


Fig.3.3.3 Analysis of the standard deviation between individual radiosonde temperatures and the average of four radiosondes computed for 6 days from the WMO High Quality Radiosonde Comparison, Mauritius, 2005. Radiosonde measurements separated by 3 to 4 hours.

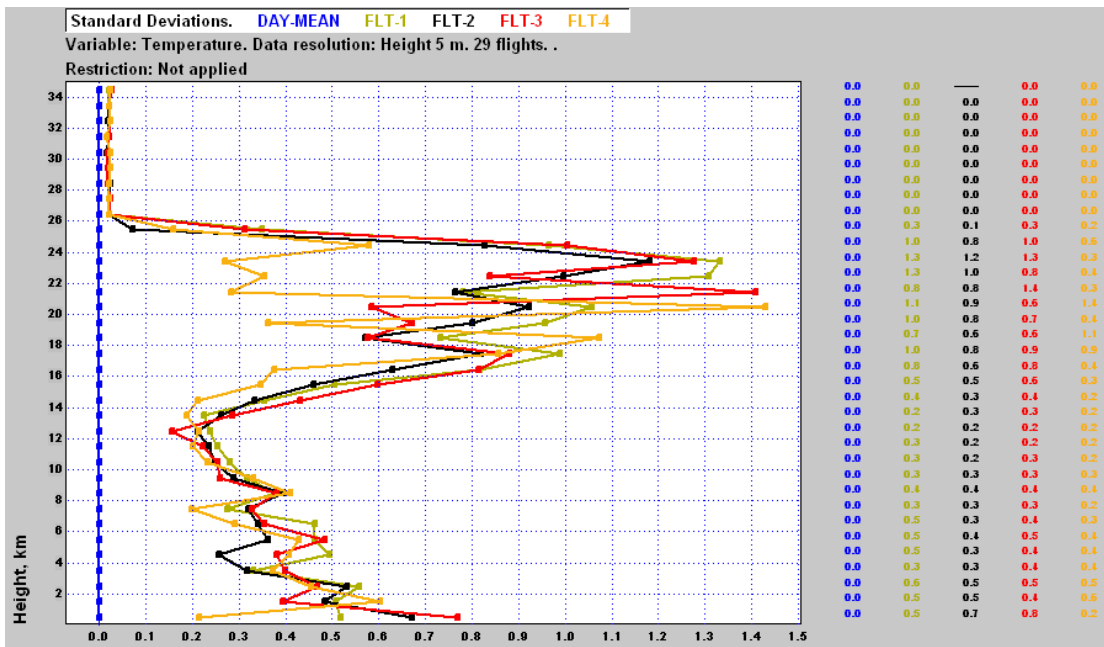


Fig.3.3.4 Analysis of the standard deviation between individual radiosonde temperatures and the average of four radiosondes computed for 5 days obtained by the UK Met Office, Dar-es-Salaam, Tanzania Internet radiotheodolite System Evaluation. Radiosonde measurements separated by 2 to 3 hours

In comparison in Fig.3.3.5, equivalent results from Camborne UK show that representativeness errors in mid-latitudes were generally about 0.5 K but with higher values in the layer immediately above the tropopause.

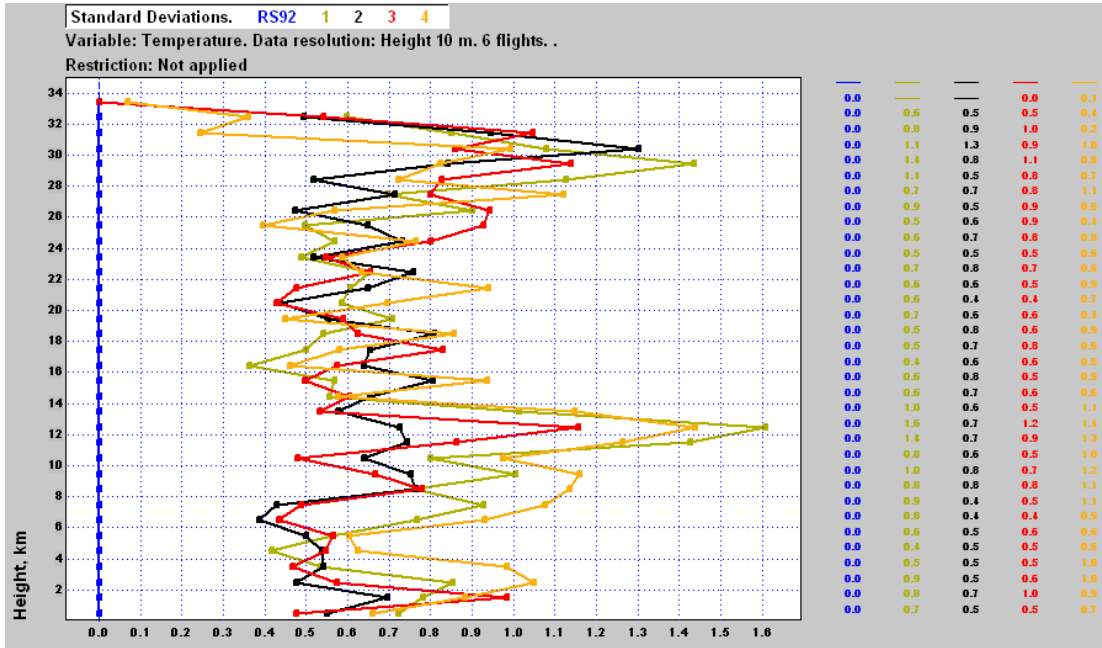



Fig.3.3.5 Analysis of the standard deviation between individual radiosonde temperatures and the average of four radiosondes computed for 6 days from a Vaisala RS92 radiosonde test at Camborne, 2004, radiosonde ascents separated by about 3 hours.

In comparing measurements between radiosondes, Kitchen [1989] showed in an early representativeness study that the atmospheric variation between radiosondes launched simultaneously about 50 km apart was similar to the atmospheric variation observed between radiosondes launched from a single site separated by 4 hours. In this study we wished to validate whether the random errors in the radio occultation profiles are lower than 1 K. Collocations between radio occultation and radiosondes were chosen so that observations were within 1 hour of nominal radiosonde launch time, so that the radiosonde representativeness errors in the troposphere because of temporal differences should have been about 0.5K or less in the tropics.

Representativeness errors caused by location differences were minimised by interpolating between a group of radiosonde measurements rather than comparing directly with individual radiosonde measurements, given the GPS profile measurements are spread in the horizontal.

4. Can the operational radiosonde network be used to validate GPS radio occultation products?

As noted in section 3, the fundamental quality of operational radiosonde temperature measurements, especially since new better quality radiosondes are being introduced in most areas of the world, is quite adequate for validating the GPS radio occultation products. However,

Ref: SAF/GRAS/DMI/REP/VS8/001 Issue: Version 1.0 Date: 23 May 2008 Document: VS8-report_18-04-08_v10.doc	GRAS Meteorology SAF Document	EUMETSAT DMI ECMWF IEEC Met Office	 www.grassaf.org
---	----------------------------------	--	--

the nature of the representativeness errors in the radiosonde sample need to be taken into account when designing validation experiments and it seems essential to have groups of high quality radiosondes rather than just individual sites.

The main problem with the sampling provided by the operational systems, see Part II, is that the collocation rate achieved with observations purely at 00 and 12 UTC is really not high enough. So this means that if groups of radiosonde stations are identified as a suitable validation area, funding would need to be provided to launch radiosondes specifically to collocate in time with a given occultation event in the area.

The results in Part II also imply that the ECMWF model background forecast in the tropics does not offer an error free reference against which to validate the GPS products, so some investment in radiosonde ascents might offer some better evidence as to the absolute accuracy of the products,


Validation of the GPS relative humidity measurements is much more problematic, with much larger data sets required and use of the detailed radiosonde archives rather than the poor resolution TEMP reports. The new generation of radiosondes, including the Vaisala RS92 have more accurate relative humidity sensors and these should be able to deliver a measurement quality that is suitable for validating GPS humidity measurements in the middle and lower troposphere, e.g. see Nash et al [2006].

5. Recommendations for the future

For validation of GPS products using radiosonde measurements it is recommended that a collocation policy of observing within 1 or at most 2 hours of the occultation event is adopted and that groups of radiosondes are used for the comparison with at least one of the radiosonde ascents within 100 km of nominal tangent point. For relative humidity evaluations a group of radiosondes with spacing of about 200 km at most would be beneficial, which might require some investment in new sites in the chosen location, or the use of temporary radiosonde sites for a given field experiment. It is relatively easy to establish temporary radiosonde sites as long as there is a suitable supply of lifting gas available. The radiosonde groupings used in Part II seem to provide a suitable basis for further validation in future, given that funding is made available for additional ascents, when necessary.

Currently many of the radiosonde stations in the tropics do not measure to high levels because the balloons used do not ensure measurements to high altitudes. This can be because they are too small, too old or too cheap. So some investment in consumables to improve the performance of the operational network might provide a good return in terms of improved data coverage in the lower stratosphere. The radiosondes used now are perfectly capable of delivering reliable measurements at these altitudes.


Radiosonde stations that are likely to have good archives are those which are nominated as part of the GCOS Upper Air Network, GUAN. So this study has relied quite heavily on observations from some of these sites in west Africa. It should be possible to get full resolution radiosonde profiles, with vertical resolution better than 20 m for temperature from these sites.

Ref: SAF/GRAS/DMI/REP/VS8/001 Issue: Version 1.0 Date: 23 May 2008 Document: VS8-report_18-04-08_v10.doc	GRAS Meteorology SAF Document	EUMETSAT DMI ECMWF IEEC Met Office	 www.grassaf.org
---	----------------------------------	--	--


In future, GCOS are also planning for a GCOS Reference Upper Air Network [GRUAN], consisting of sites with high quality radiosondes, a possible collocation strategy with satellite measurements and a range of ground based remote sensing to support the radiosonde measurements. Pilot stations for this network should also be available for validation of GPS radio occultation products within a few years. At this time the lead scientific team for this work will be based at Lindenberg Observatory, Deutsche Wetterdienst.

References

- G.A.Hajj, Kursinski, E.R., Romans, L.J., Bertiger, W.I. and Leroy, S.S. [2002] A Technical description of atmospheric sounding by GPS occultation. *J. Atmos. Solar-Terr. Phys.*, 64(4),451-469.
- S.B.Healey, Eyre, J.R., Hamrud, M. and Thépaut, J-N [2006] Assimilating GPS radio occultation measurements with two-dimensional bending angle observation operators. *Q. J. R. Meteorol. Soc.* **133**, pp.1213-1227.
- A.A. Ivanov, Kats, A., Kurnosenko, S., Zaitseva, N. and Nash, J. [1991] WMO International Radiosonde Comparison- Phase III, Dzhambul (USSR). *WMO Instrument and Methods of Observation Report* No.40, WMO/TD 451
- M. Kitchen,[1989] Representativeness errors for radiosonde observations. *Q. J. R. Meteorol. Soc.* **115**, pp.673-700.
- E. Kursinski , Hajj,G., Schofield , J., Linfield, R. and Hardy, K. [1997] Observing earth's atmosphere with radio occultation measurements using the Global Positioning System, *J. Geophys. Res.*, **102**, pp. 23,429-23465.
- J. Nash [1994] Comparison of potential reference radiosonde observations ; results from PREFRS-92. Wmo Technical Conference on Instruments and methods of Observations (TECO-94), Geneva 1994. WMO/TD –No 588, pp 115-119.
- J. Nash , Smout, R. , Oakley, T.J., Pathack, B., and Kurnosenko, S. [2006] The WMO Intercomparison of Radiosonde Systems- Final Report. Vacoas, Mauritius 2-25 February 2005. *WMO Instrument and Methods of Observation Report* No.83, WMO/TD 1265.
- J. Nash and Schmidlin, F.J. [1987] WMO International Radiosonde Comparison, UK 1984 and USA 1985. *WMO Instrument and Methods of Observation Report* No.30, WMO/TD 195.
- C. Reigber , Schwintzer, P., Lühr, H. and Wickert, J. [2005] Earth Observation with CHAMP :Results from Three Years in Orbit, *Springer Verlag*, 2005.
- J. Wickert , [2004] Comparison of vertical refractivity and temperature profiles from CHAMP with radiosonde measurements. Danish Meteorological Institute, Scientific Report 04-09.

Ref: SAF/GRAS/DMI/REP/VS8/001 Issue: Version 1.0 Date: 23 May 2008 Document: VS8-report_18-04-08_v10.doc	GRAS Meteorology SAF Document	EUMETSAT DMI ECMWF IEEC Met Office	 www.grassaf.org
---	----------------------------------	--	--

S. Yagi, Mita, A., and Inoue, N. [1996] WMO International Radiosonde Comparison - Phase IV, Tsukuba (Japan) 1993 Final Report. *WMO Instrument and Methods of Observation Report No.59*, WMO/TD 742.

Ref: SAF/GRAS/DMI/REP/VS8/001 Issue: Version 1.0 Date: 23 May 2008 Document: VS8-report_18-04-08_v10.doc	GRAS Meteorology SAF Document	EUMETSAT DMI ECMWF IEEC Met Office	 www.grassaf.org
---	----------------------------------	--	--

Part II Temperature and Humidity profile comparison between Radiosondes and GPS radio occultation observations

Mark Smees

Met Office, Exeter, UK

February 2007

Introduction

The GNSS (Global Navigation Satellite System) Receiver for Atmospheric Sounding (GRAS) Meteorology Satellite Application Facility (SAF) is a EUMETSAT-funded project, which is developing an operational GPS radio occultation system. It is responsible for delivering temperature, pressure, and humidity profiles in real time, software products for numerical weather prediction models and for carrying out related research. The GRAS SAF is led by the Danish Meteorological Institute (DMI), with partners the Met Office and the Institut d'Estudis Espacials de Catalunya (IEEC). During 2006 GRAS SAF was tasked with conducting a Radio Occultation Processing Intercomparison Campaign (ROPIC), comparing radiosonde data with satellite temperature and humidity profiles.

For this initial evaluation, satellite data and radiosonde ascents were compared using the RSKOMP radiosonde comparison software, as written by S. Kurnosenko primarily for processing WMO Radiosonde Comparison results.

Area selection process

In considering the processed results, the earth was divided into three regions; latitudes above 60° north and south, mid-latitudes between 30° and 50° north and south, and lastly the Tropics between 30° north and south. At least 3 areas with a group of radiosondes close together were selected for each of these region. The criteria used for selecting the radiosonde stations in each group was; a minimum of 4 sonde stations for each area, all flying the same radiosonde type, preferably with ascents at 00UTC and 12UTC, and with as many flights as possible reaching 50hPa or higher. The radiosonde stations were selected using the UaS-tats_Quarterly2005.xls spreadsheet, compiled by the CIMO Rapporteur on Radiosonde Compatibility, Tim Oakley, UK Met Office.


Data used for comparisons

GPS radio occultation Satellite data

Satellite data files were received from Peter Thejll at DMI, these data files were from a 1dvar retrieval, using ECMWF model fields. These data were a mixture of RO observations as influenced by the model background/data for temperature, pressure and humidity, (i.e., the comparison is comparing radiosondes with partly model and partly data. Each satellite file contained the derived profiles of temperature and humidity versus height. With the header information indicating, date, time and location of the profile, as well as the identity of each column.

Satellite profile times and locations are shown in Table 2 Satellite and Radiosonde locations and profile times in [annex A](#).

Radiosonde data

Ref: SAF/GRAS/DMI/REP/VS8/001 Issue: Version 1.0 Date: 23 May 2008 Document: VS8-report_18-04-08_v10.doc	GRAS Meteorology SAF Document	EUMETSAT DMI ECMWF IEEC Met Office	 www.grassaf.org
---	----------------------------------	--	--

The Radiosonde data were retrieved from the University of Wyoming web site at <http://weather.uwyo.edu/upperair/sounding.html>

A list of radiosonde launch time and location is shown in Table 2 Satellite and Radiosonde locations and profile times in annex A

A list of the radiosonde equipment used at each station can be found in Table 3 Radiosonde equipment in Annex B.

The radiosondes in each area were from the same manufacturer. Some of the radiosonde flights do not reach a great altitude. Some comparisons have a limited number of radiosonde with which to compare, also some radiosonde flights did not have TEMP part B, therefore the profile was plotted using the standard levels from TEMP part A.

The performance of different type of radiosonde can be found in the WMO Instruments and observing methods report No. 80 the “WMO Catalogue of Radiosondes and Upper-Air Wind Systems in use by Members in 2002 and Compatibility of Radiosondes Geopotential Measurements for period from 1998 to 2001” by John Elms, UK Meteorological Office, at <http://www.wmo.ch/web/www/IMOP/publications-IOM-series.html>

Maps of Areas

The maps in [annex D](#) show the location and distance between the radiosonde stations and the approximate location of the satellite profiles.

Data processing


Satellite data was converted from ASCII file format to a comma separated file format using an excel spreadsheet; this enables it to be used by the RSKOMP radiosonde comparison software. As the height in the satellite file was in kilometres an extra column was added to convert the height to meters. Also the humidity (g/Kg) column, was copied and added as an extra column, called mixing ratio, thus enabling them to be compared with the radiosonde mixing ratio.

The raw radiosonde temp message was used to identify the type of radiosonde, the processing equipment, solar radiation correction and the time of launch. The ASCII text file containing selected point information was downloaded and opened in an excel spreadsheet. This was then modified and saved as a comma separated file to enable it to be used by the RSKOMP radiosonde comparison software. An extra column was added to the radiosonde data, to convert the temperature data from degrees centigrade to degrees Kelvin.

The RSbest data was obtained by interpolating the distance from the radiosonde stations and the satellite profile, a weighting factor was then applied to each radiosonde ascents. This weighting factor can be found as the RSbest %, in [Table2 Satellite and Radiosonde locations and profile times](#), at [annex A](#). An extra dataset RSbest+ has been added, this dataset has an extra column added. This column is a copy of the radiosonde temperature column, however in the RSK dataset it has been called Model Temperature. The satellite model temperature is taken from column 3 in the satellite files, i.e. the ECMWF profile temperature. This allows us to compare the satellite model temperatures against the best fit radiosonde temperature, using the RSK statistical software.

Comparisons.

48 satellite profiles have been received, and radiosonde flights have been downloaded for comparisons of these satellite data. Of these 48 comparisons; 10, 16, 18 and 44, have been

Ref: SAF/GRAS/DMI/REP/VS8/001 Issue: Version 1.0 Date: 23 May 2008 Document: VS8-report_18-04-08_v10.doc	GRAS Meteorology SAF Document	EUMETSAT DMI ECMWF IEEC Met Office	 www.grassaf.org
---	----------------------------------	--	--

excluded from the dataset, as they produce outliers, outside of what we normally expect. See [annex E](#) for an explanation why these comparisons were excluded. This leaves 44 comparisons; 15 in the High latitudes region, those greater than 60° Latitude; 10 in the mid latitudes region, between 30° and 60° north and south; and 19 in the Tropics region, 30° either side of the equator. The High latitude region has been divided into, profiles in Greenland and the others. Greenland is being considered as a separate case, therefore there are 10 good profile in the Greenland comparison and 5 good profiles for the rest of the high latitude profiles.

Collocation Considerations.

Radiosonde balloons ascend at approximately 1000 feet per minute, therefore a radiosonde will take approximately, 65 minutes to reach 20km, and 100 minutes to reach 30km. Apart from the comparisons in Europe, I have not taken in to account the weather conditions.

The latitude and longitude in the received satellite profiles are only one of several possible representations of the profile latitude and longitude on its way down through the atmosphere. The profile from a radio-occultation is not a straight line, but it still has to have some value for latitude and longitude. The one reported relates to the position on the surface of the Earth of a point created as the midpoint of a certain line segment which is defined on the line between two satellites at the last instant when data were received. The signals from the GPS transmitters do not move in a straight line from satellite to satellite, due to refraction processes in the ionosphere and atmosphere. Imagine connecting the two satellites by a straight line at the moment the last signal is received before the Earth occults the satellites. That straight line bisects the WGS-84 ellipsoid - or the Earth's surface. Between the point of entry and the point of exit of this imaginary line through the atmosphere we have a line segment. Find the middle of that line and project it up to the surface of the WGS-84 ellipsoid (or the Earth's surface). The latitude and longitude of that point is what is reported as the latitude and longitude in the satellite profile. The time taken for a satellite to make one measurement is in the order of a few tens of seconds, depending on the heights at which the signal is first obtained and subsequently lost.

Temperature evaluation.

The statistics produced show the flight-by-flight differences (left plot) and the flight-by-flight standard deviations (right plot) as a function of height, with the temperature in degrees Kelvin. Direct differences are the results of taking all the samples in a given category [each 10m in the vertical] and computing the average value for the difference and the standard deviation. In flight by flight differences, differences for a given collocation (comparison) are averaged for a given category and then the individual averages are combined to estimate the overall average and the flight by flight standard deviation.

In the following temperature statistics graphs, the best fit radiosonde (link reference) temperature is the yellow trace, and the satellite temperature is the blue trace. The Y axis is height from 0 to 35km, and the red numbers on the graph are the corresponding sample sizes.

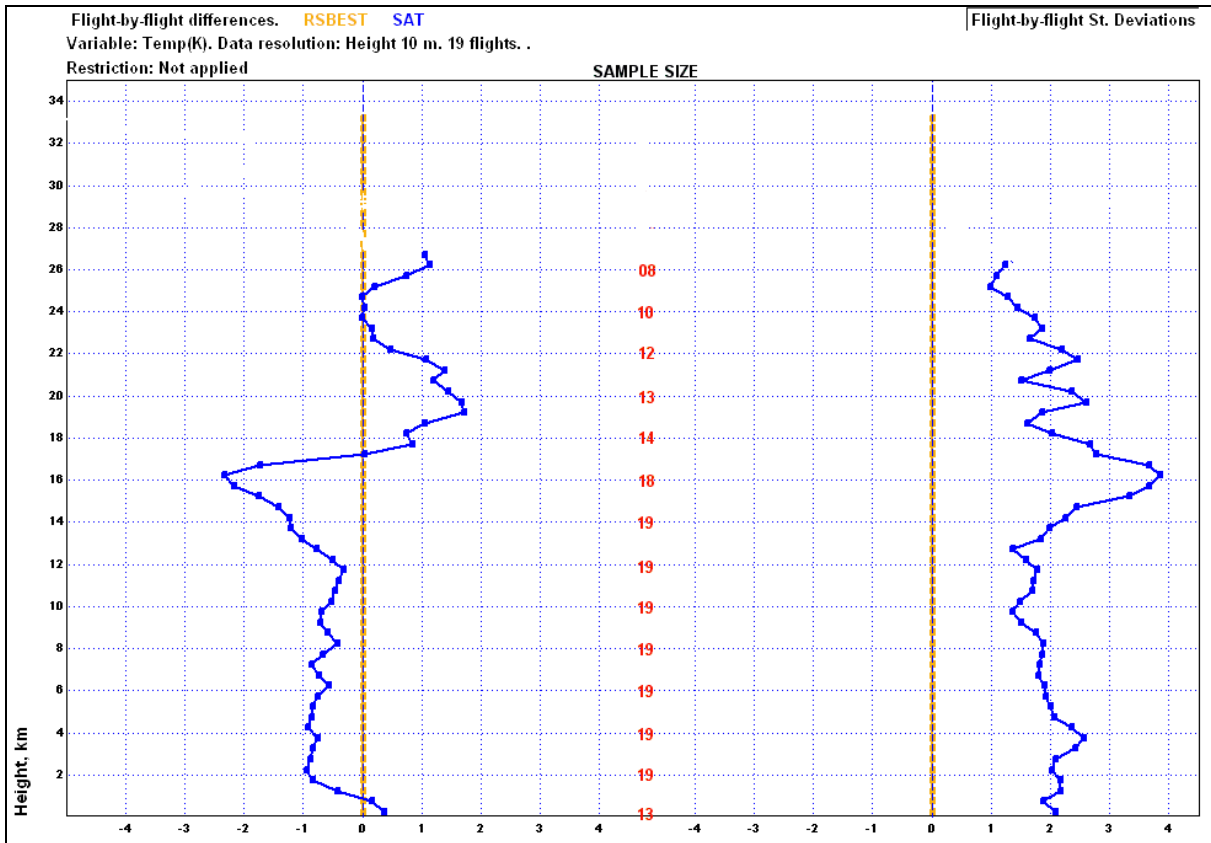


Figure 1 Flight-by-flight differences and Flight-by-flight Standard Deviations for the Tropics Temperature comparison [little difference between standard deviations and flight by flight standard deviations.]

The larger standard deviation seen in Figure 1 around the tropopause (16km) can be explained by two satellite profiles in comparisons 33 and 35. If we remove these comparisons from the dataset, this larger deviation is removed, see Figure 2 below. The reason comparisons 33 and 35 create a larger deviation is their tropopause temperature is much colder than the radiosonde soundings, see Figures 3 and 4 for these satellite and radiosonde profiles. . In these figures the Y axis is height from 0 to 30km, and the X axis is temperature in Kelvin. The blue trace is the satellite profile, and the other three are the radiosonde ascents.

In both Fig. 3 and 4 , the temperature perturbations of the satellite measurements relative to the radiosondes are strongly negative from below the tropopause with peak positive perturbations at about 3 km and 8 km above the maximum negative difference. It is unclear whether this could be the result of an extremely strong gravity wave [positive vertical velocity anomaly near the tropopause] seen by the satellite and not the radiosondes, but the amplitude of the differences was very much larger than any seen in earlier radiosonde testing in Africa. There are not usually large temperature differences in the horizontal in the upper troposphere in the tropics. In an ideal situation the west African radiosonde network would benefit from more measurement sites and then it would be easier to resolve these issues. It was also noted that the cost functions for these two profiles were high indicating large differences from the ECMWF background fields

Certainly the satellite profile in Fig.4 looks a bit suspicious, because it is colder than the radiosondes at nearly all levels, with this magnitude of difference relatively uncommon in the tropics, and leading to significant geopotential height anomalies at 100 hPa.

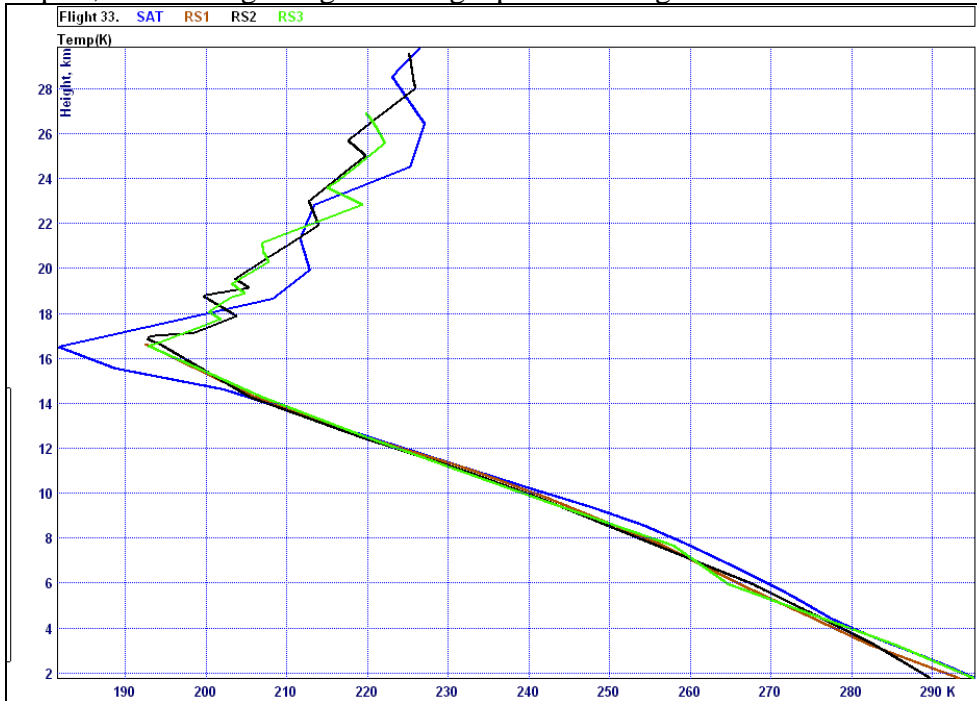


Figure 3 Comparison 33 satellite tropopause temperature colder than the radiosonde profiles.

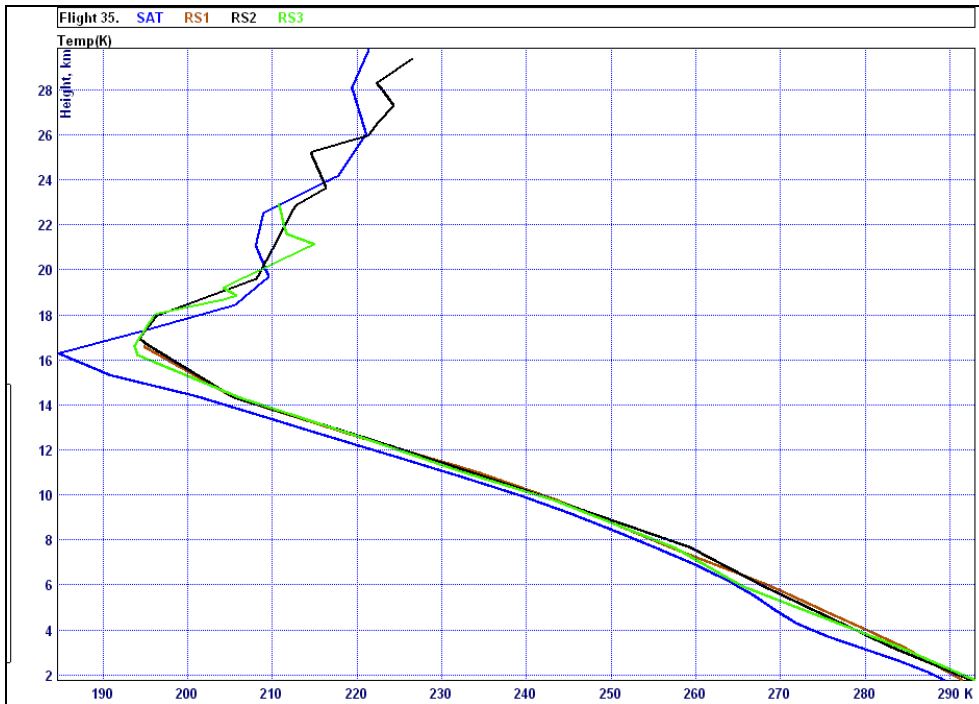


Figure 4 Comparison 35 satellite tropopause temperature colder than the radiosonde profiles.

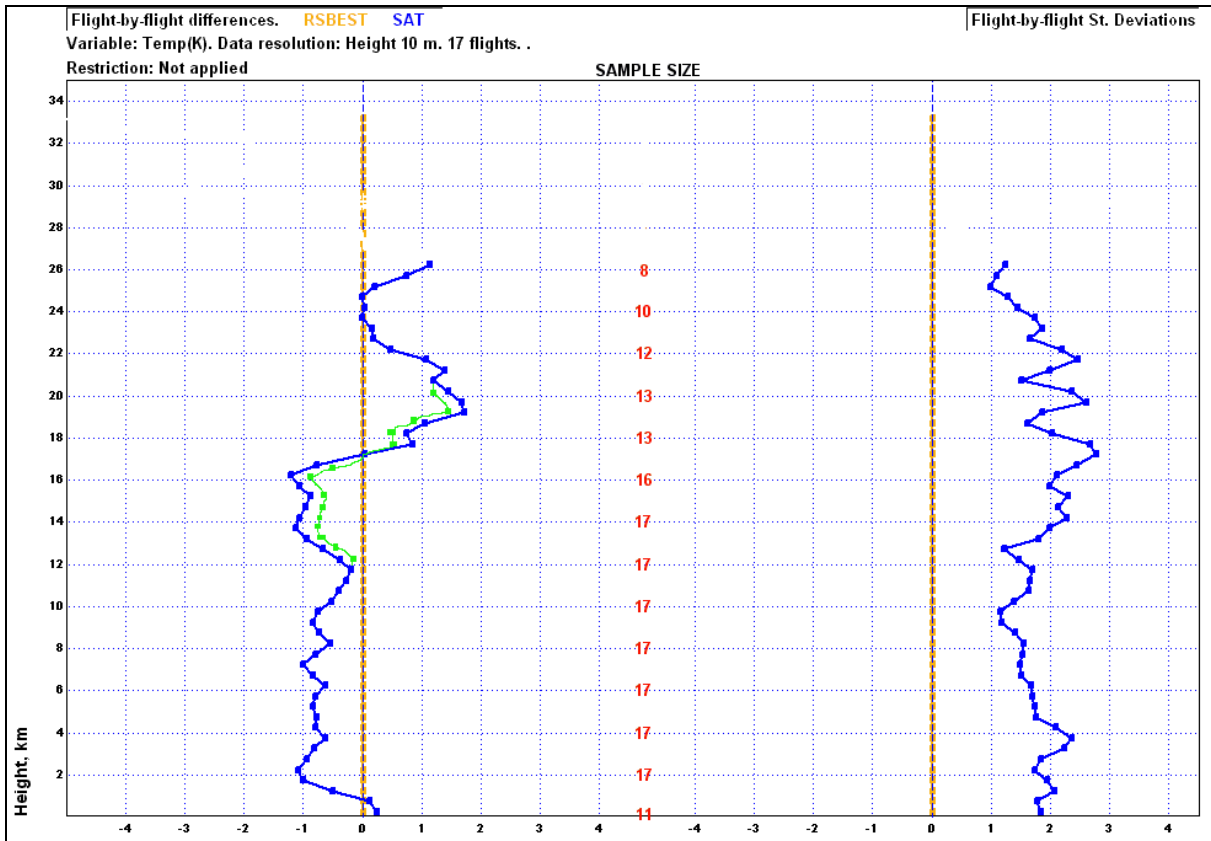


Figure 2 Flight-by-flight differences and Flight-by-flight Standard Deviations for the Tropics Temperature comparison, with comparisons 33 and 35 removed.

In the tropics the sign of the bias changes after the tropopause, as can be seen in Figure 2. This is probably because there may be a difference between the GPS and the radiosonde heights. Radiosonde comparison test have demonstrated that the greatest radiosondes pressure error with this type of radiosonde at the tropopause is no greater than 1hPa. Between 150 and 100 hPa, a 1 hPa error would lead to a temperature offset of 0.23 degrees in the tropics. In Figure 2, the green line represents the change to the comparison caused by a radiosonde error of -1 hPa. Thus, the temperature differences could be caused by a height difference of between 200 and 300m in the measurements, with the satellite measurements lower than the radiosondes.

If a more strict spatial location criteria is applied so only occultations with one radiosonde close to the tangent point are considered, the results of the collocation statistics are almost exactly the same as in Fig. 2 but with the data set only containing 12 collocations.

The most reliable agreement between the radiosondes and the GPS occultations in terms of random errors occurs in the upper troposphere in the tropics where the radiosonde representativeness and coding errors are smallest, but even here the random errors in the GPS measurements do not appear to be lower than 1K. The higher standard deviations closer to the surface are probably mostly due to poorer quality GPS measurements.

Figures 5 and 6 below show the statistics for the GPS occultation temperature and the satellite model temperature for the Tropics region, with the radiosonde as the link reference. Displayed are the flight-by-flight differences (left plot) and the flight-by-flight standard deviations (right plot), computed as a function of height. The satellite temperature, blue trace and model temperature, red trace are in degrees Kelvin. Figure 5 includes comparisons 33 and 34 and in figure 6, they are excluded. The model background does not agree particularly well with the radiosondes, but has a strong similarity to the GPS occultation products with respect to systematic bias. The two suspicious occultation products [very cold tropopause] were clearly not present in the NWP forecasts.

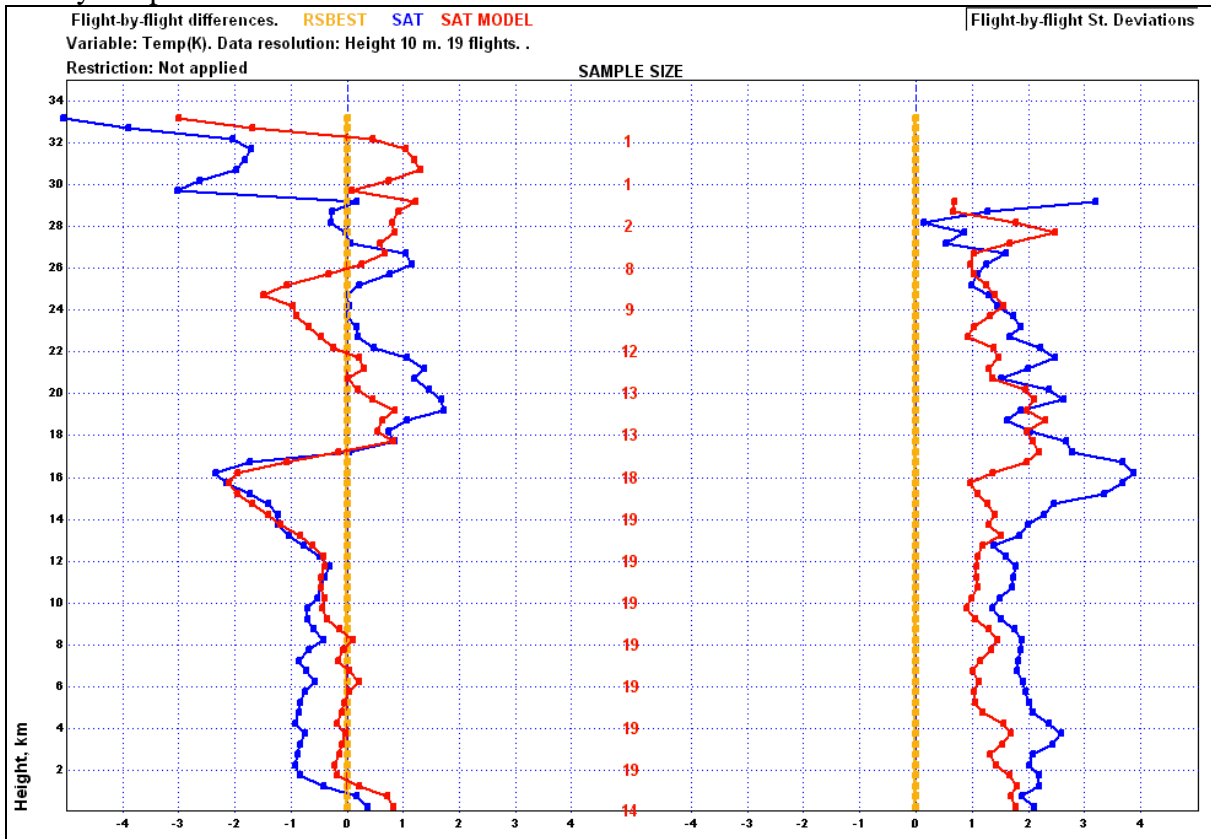


Figure 5 Tropics region Flight-by-flight differences and Flight-by-flight Standard Deviations for the Satellite Temperature and Satellite Model Temperature comparisons, including comparison 33 and 35

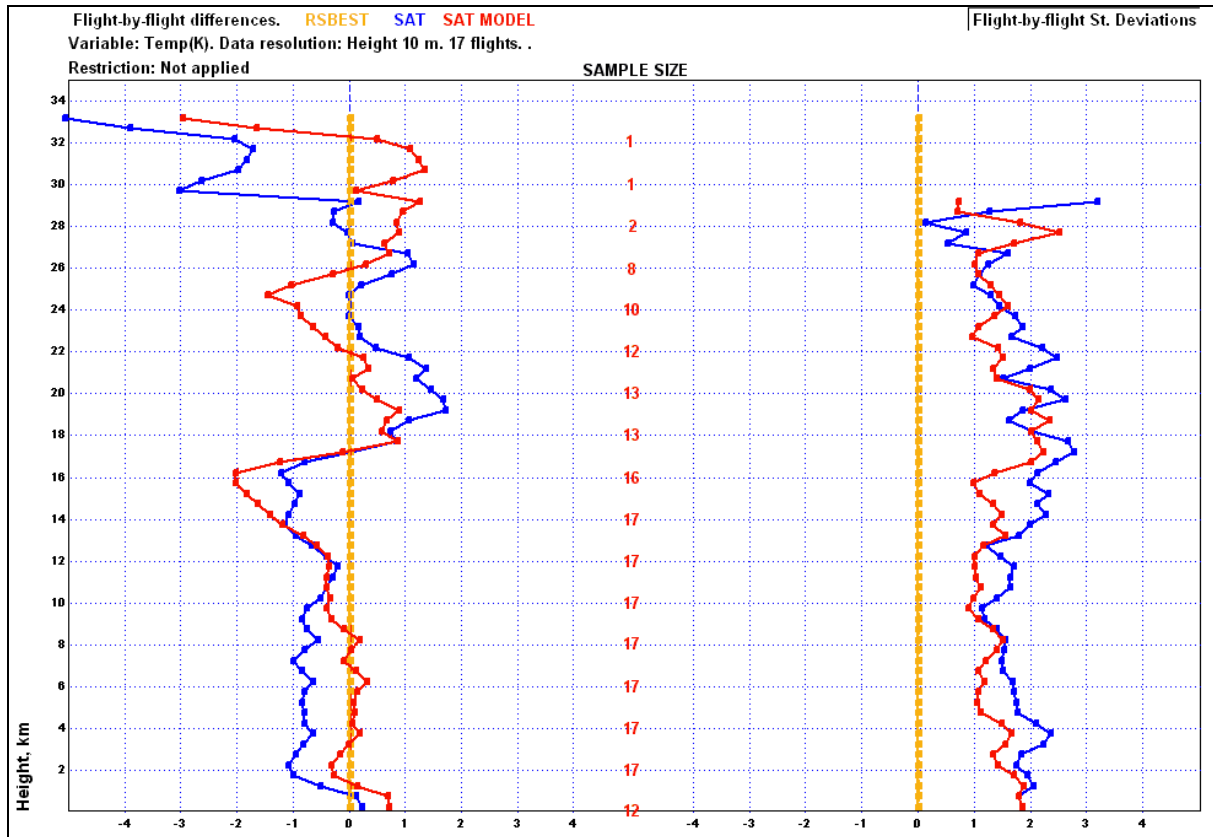


Figure 6 Tropics region Flight-by-flight differences and Flight-by-flight Standard Deviations for the Satellite Temperature and Satellite Model Temperature comparisons, excluding comparisons 33 and 35.

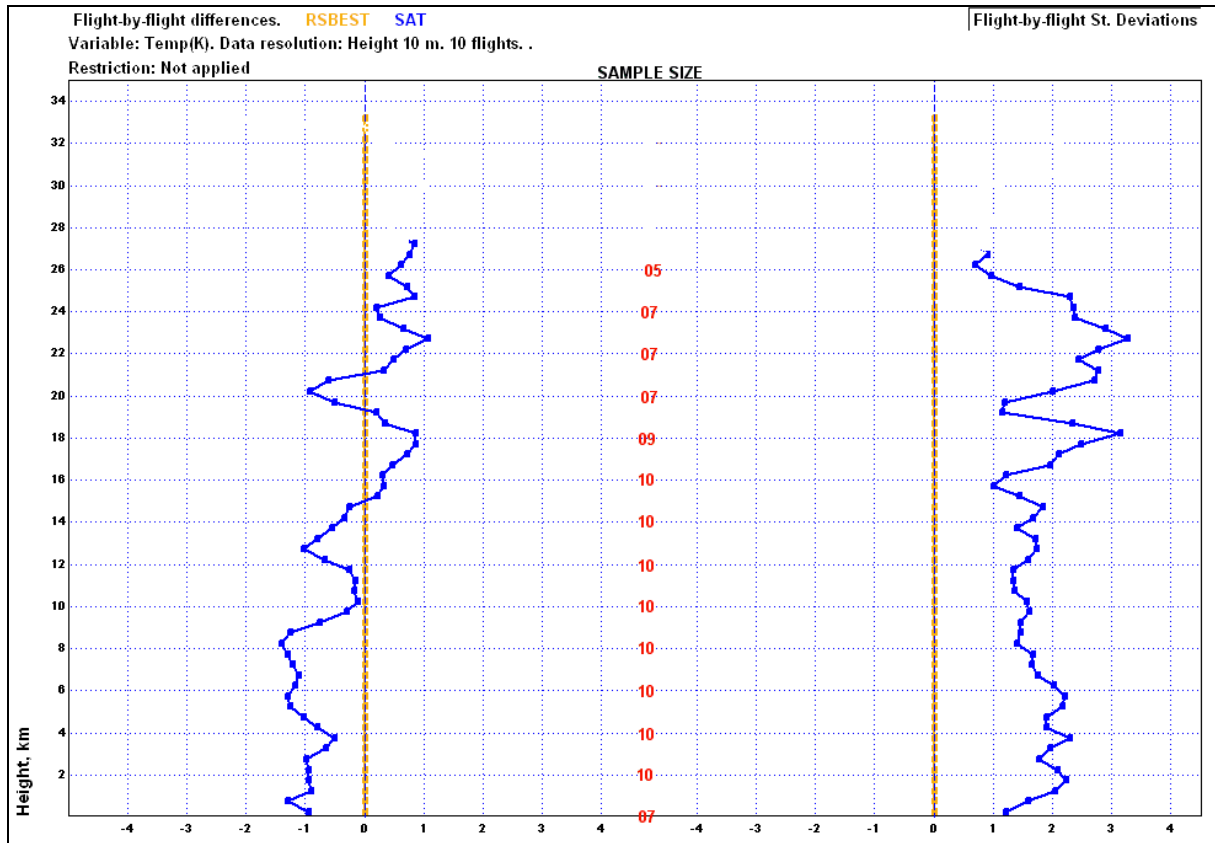


Figure 7 Flight-by-flight differences and Flight-by-flight Standard Deviations for the Mid-Latitude Temperature comparisons.

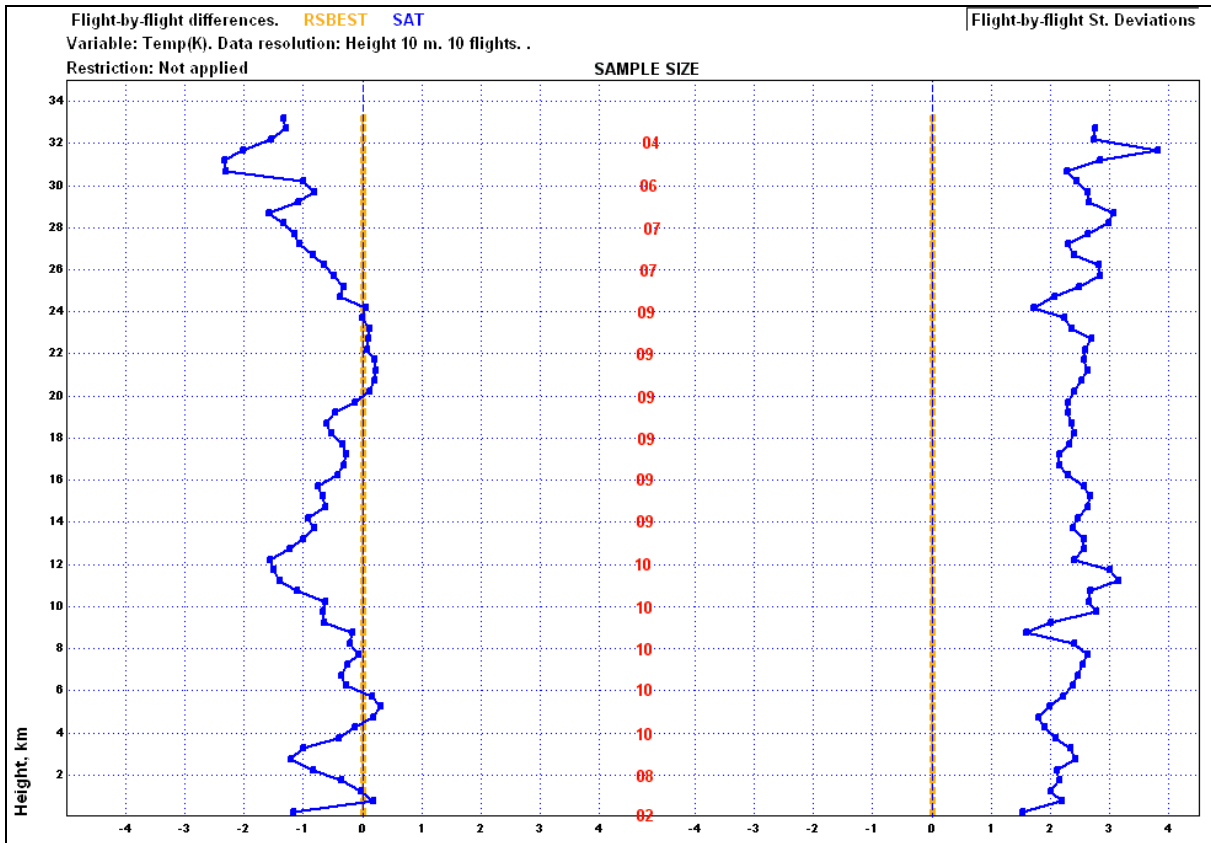


Figure 8 Flight-by-flight differences and Flight-by-flight Standard Deviations for the Greenland Temperature comparisons.

The collocation data sets for midlatitude and Greenland were too small to infer very much. The midlatitude data set has standard deviations which were similar to the upper troposphere in the tropics. The standard deviations around Greenland were larger and this probably reflected that local variation in temperature fields around the Greenland ice cap were too large to provide a good basis for evaluating GPS radio occultation measurements.

Humidity evaluation.

For the humidity evaluation, statistics have been produced to show the flight-by-flight differences (left plot) and the flight-by-flight standard deviations (right plot) for each of the regions. The humidity is expressed as a mixing ratio in grams per kilogram (g/kg), X axis, and the height resolution applied is every 10 metres. In figures 9 to 12, the best fit radiosonde (link reference) mixing ratio (humidity) is the yellow trace, the Satellite humidity is the blue trace. The Y axis is height from 0 to 18km, and the red numbers on the graph are the corresponding sample sizes. Where the sample size was less than 3, the satellite humidity trace has been removed from the graph.

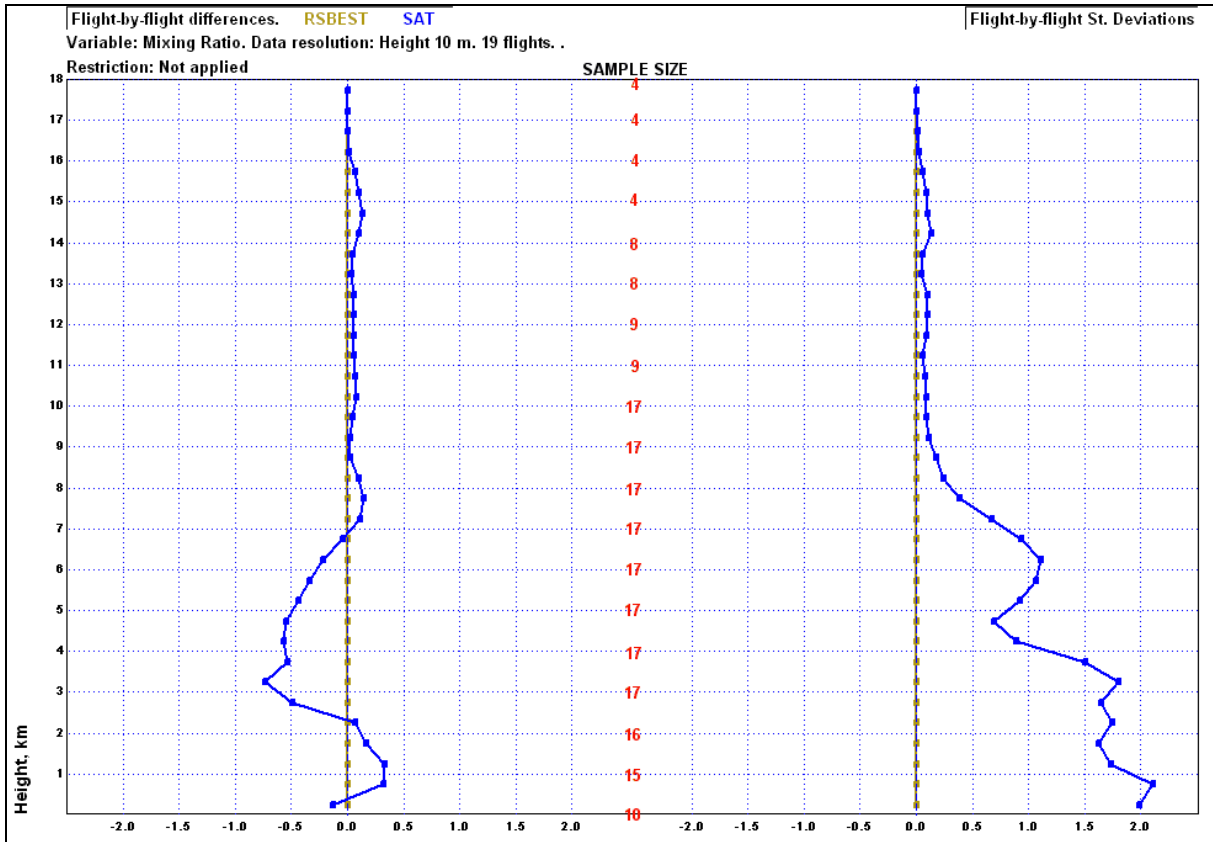


Figure 9 Flight-by-flight differences and Flight-by-flight Standard Deviations for the Tropics Humidity comparisons.

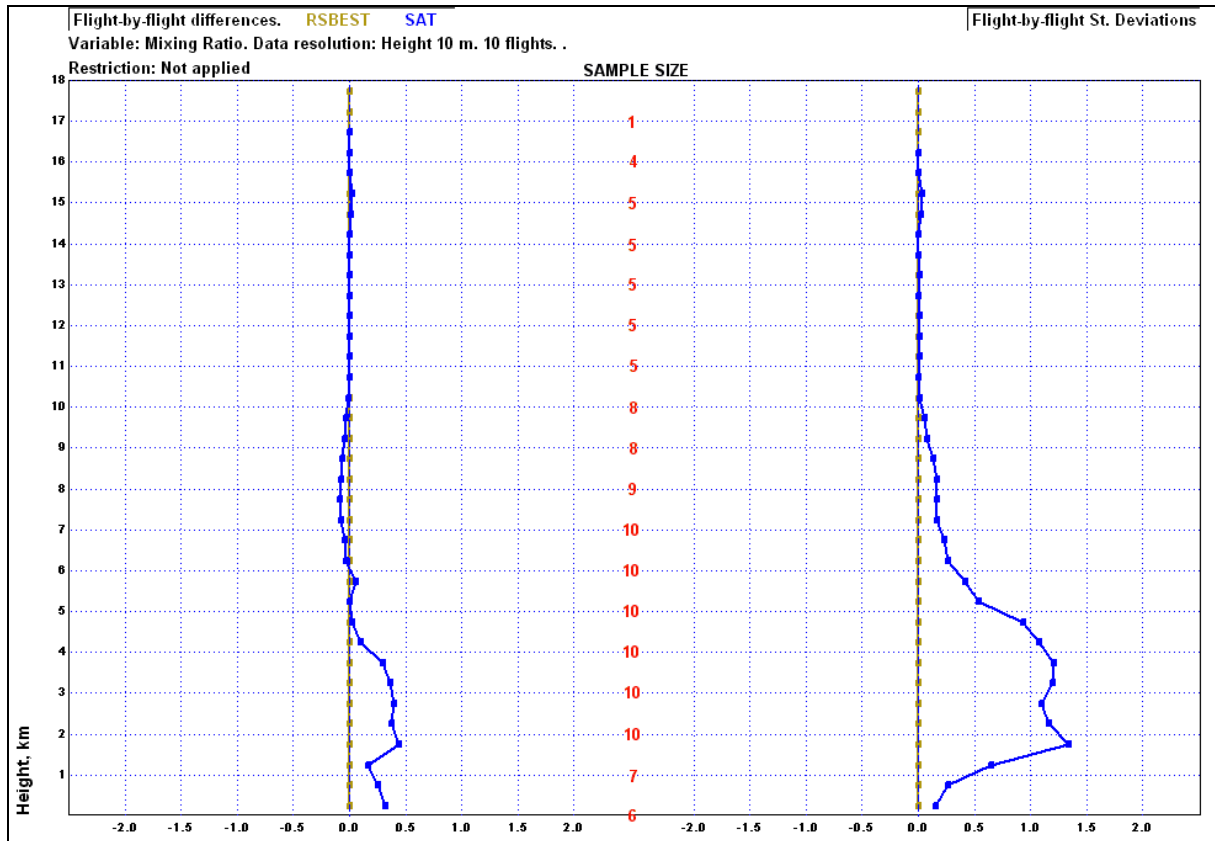


Figure 10 Flight-by-flight differences and Flight-by-flight Standard Deviations for the Mid-Latitude Humidity comparisons.

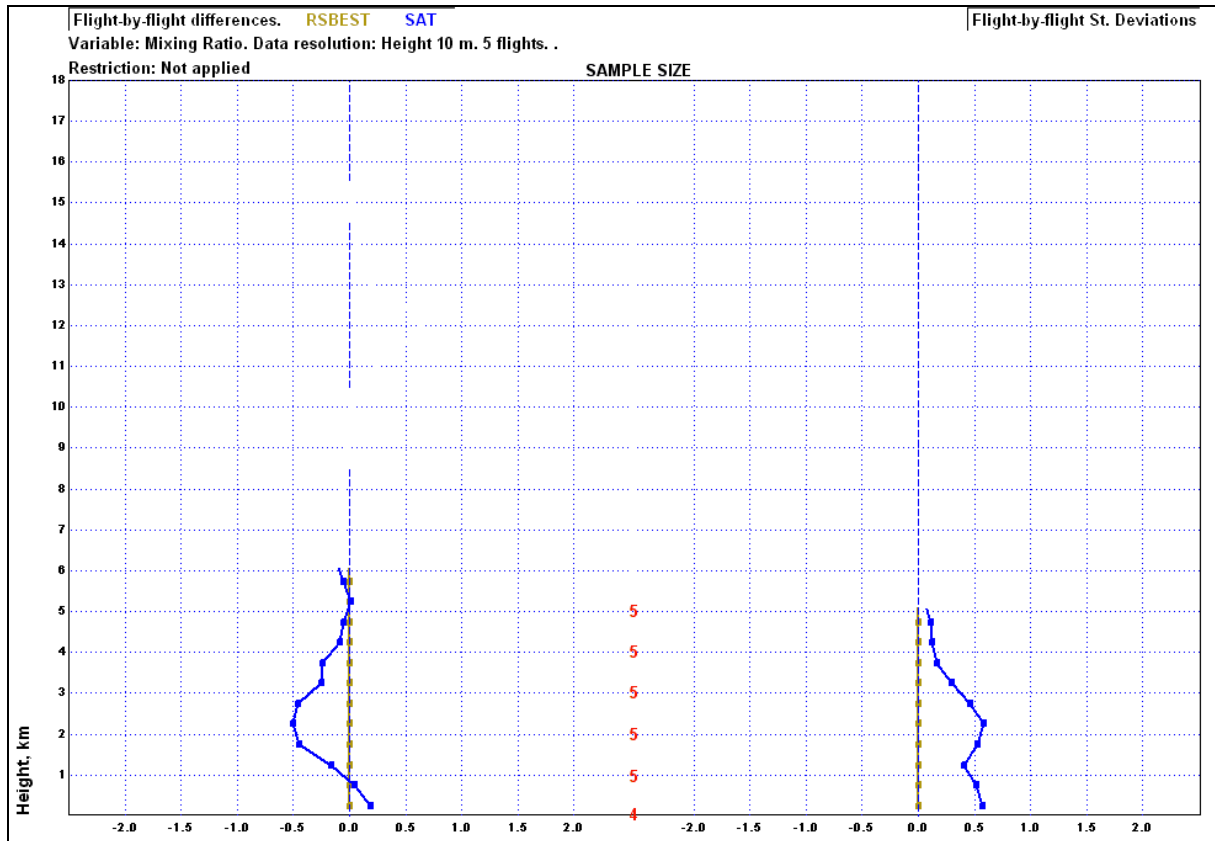


Figure 11 Flight-by-flight differences and Flight-by-flight Standard Deviations for the High-Latitudes Humidity comparisons.

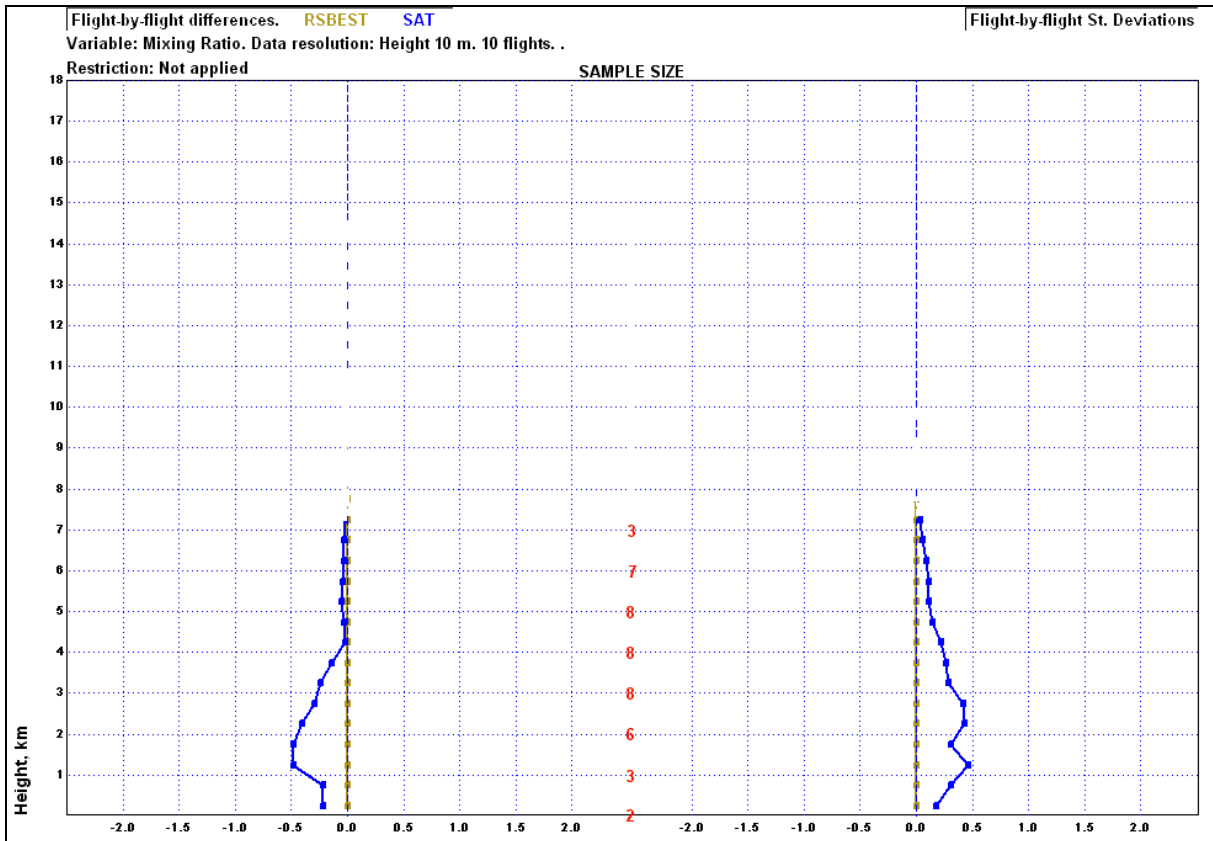


Figure 12 Flight-by-flight differences and Flight-by-flight Standard Deviations for the Greenland Humidity comparisons.

Examples of Individual comparisons

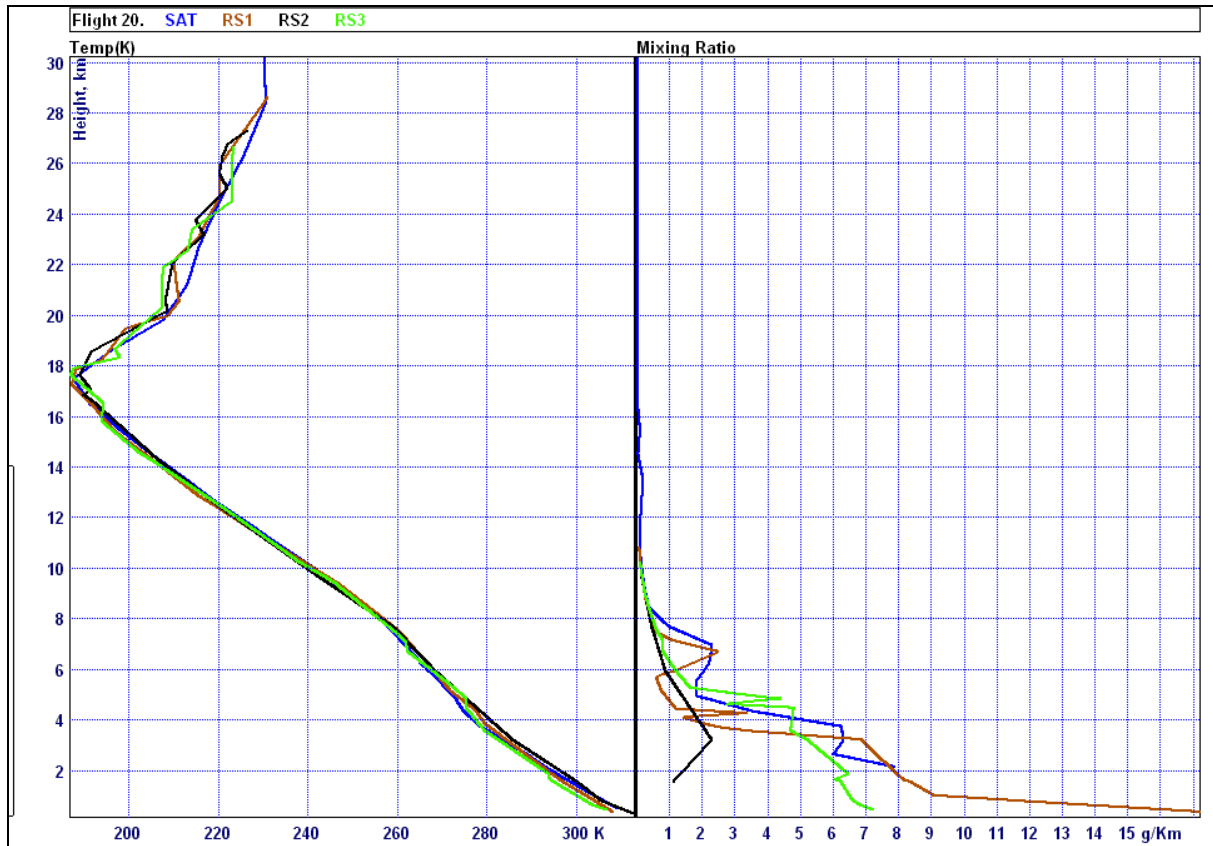


Figure 13 comparison 20.

Shown in figure 13 above is comparison 20, from the Tropics (West Africa) consisting of the satellite profile in blue and 3 RS80 radiosonde ascents. The Y axis is height from 0 to 30km, and the X axis is temperature (K), in the left window, and mixing ration (g/Kg), in the right window. This shows an ascent where all the radiosonde and satellite temperature profiles are very close, however the humidity (mixing ratio) is vastly different.



Figure 14 Comparison 15

Shown in figure 14 above, are 4 radiosonde ascents from Germany and the satellite profile in blue, for comparison 15. It can be seen that the 2 radiosonde ascents (RS1, brown and RS2, black traces) the nearest the satellite profile, approximately 140km away, show the top of the moistest layer significantly lower than the satellite profile, since for measurements at this level the precise depth of these layers is important. In this case the weighting factor for RS1 and RS2 is 50% to obtain the best match for the satellite profile. See figure D2 for the location of this comparison.

Summary and conclusions

Mark's notes.

1. In a year, only 48 satellite profiles were found to fall in the selected areas, of these, 4 had to be totally excluded, and some parts of the remaining radiosonde and satellite profiles had to be removed from the calculations.

Region	Number of Flights	Excluded Flights
High-Latitudes	5	0
Greenland	11	1
Mid-Latitudes	10	0
Tropics	22	3
Total	48	4


Ref: SAF/GRAS/DMI/REP/VS8/001 Issue: Version 1.0 Date: 23 May 2008 Document: VS8-report_18-04-08_v10.doc	GRAS Meteorology SAF Document	EUMETSAT DMI ECMWF IEEC Met Office	 www.grassaf.org
---	----------------------------------	--	--

Table 1 Number of radiosonde ascents

2. The method of picking areas, where there was supposedly at least 4 good radiosonde ascents, and producing a best fit profile to match the location of the satellite profile works well for temperature. However for humidity this method does not work so well, humidity over such a wide area is very variable. Also the method would work better if all radiosonde stations in the selected areas produced; Temp messages at both 00UTC and 12UTC up to a height of 5hPa, and the messages were transmitted on to the GTS. This is not the case at the moment some radiosonde stations ascents are intermittent and the quality of some ascents may be suspect.
3. It would be better if we could get high resolution radiosonde data, a 2 second ASCII file, rather than just rely on the temp messages.
4. Only some of the areas had enough satellite profiles to be able to make a suitable comparison. To increase the number of comparison; reduce the comparison time; or include other areas, it would be necessary to introduce special radiosonde ascents, of sufficient high-quality quality.
5. There are enough examples in the tropics to make a conclusion.
6. There not enough examples to draw any valid conclusions in the high latitudes.
7. The tropics temperatures are valid up to about 24km, after this the sample size is too small.
8. In the tropics the sign of the bias changes after the tropopause, possibly there may be a difference between the GPS and the radiosonde heights. See figure 2.
9. The Greenland ice cap causes a problem when comparing satellite and radiosonde profiles. Pairs of radiosonde stations are on the opposite sides of the ice cap, and as a result have a very different profile in the lower troposphere, however in the upper troposphere they may be similar. Greenland does not seem a particularly good location for collocation activities.

Ref: SAF/GRAS/DMI/REP/VS8/001
Issue: Version 1.0
Date: 23 May 2008
Document: VS8-report_18-04-08_v10.doc

GRAS Meteorology SAF
Document

EUMETSAT
DMI
ECMWF
IEEC
Met Office



Annex A

Table 2 Satellite and Radiosonde locations and profile times

No.	Date UTC	Satellite			Radiosondes. In order of distance from satellite profile, RS1 nearest.						RSbest %	Distance to nearest sonde station & Comments
		Time UTC	Lat	Long	RS No	WMO No.	Name	Time	Lat	Long		
1	6/01/2003	12:52	64.9N	11.4E	1	01241	Orland	11:09	63.7N	9.6E	50	160km. Warm front N-S across Norway.
					2	01152	Bodo	11:10	67.3N	14.4E	50	
					3	02365	Sundsvall	11:30	62.5N	17.5E	0	
2	16/01/2003	12:29	52.3N	12.8E	1	10393	Lindenberg	10:45	52.2N	14.1E	55	90km.
					2	10184	Greifswald	10:45	54.1N	13.4E	30	
					3	10035	Schleswig	10:51	54.5N	9.6E	10	
					4	10200	Emden	10:45	52.4N	7.2E	5	
3	17/01/2003	00:34	65.7N	12.8E	1	01241	Orland	23:08	63.7N	9.6E	67	190km. Warm front E-W across southern Scandinavia.
					2	01152	Bodo	23:10	67.3N	14.4E	33	
					3	02365	Sundsvall	23:30	62.5N	17.5E	0	
					4	02185	Lulea-Kallax	23:30	65.6N	22.1E	0	
4	02/10/2004	23:20	3.4N	113.4E	1	96441	Bintulu	23:38	3.2N	113.0E	60	50km. Bintulu (96441) no data between 162 and 98.8 hPa.
					2	96471	Kota Kinabalu	23:37	5.9N	116.1E	20	
					3	96481	Tawau	23:38	4.3N	117.9E	10	
					4	96413	Kuching	23:45	1.5N	110.3E	10	
5	01/01/2004	23:55	67.9N	32.9N	1	04360	Tasiilaq	23:20	65.59N	37.63W	40	330km. Warm front to the east of Greenland.
					2	04339	Ittoqqortoormiit	23:00	70.48N	21.95W	30	
					3	04220	Aasiaat	23:29	68.69N	52.84W	20	
					4	04270	Narsarsuaq	23:00	61.15N	45.43W	10	
6	06/01/2004	23:41	16.4N	64.7W	1	78526	San Juan	23:06	18.45N	66.00W	100	260km.

No.	Date UTC	Satellite			Radiosondes. In order of distance from satellite profile, RS1 nearest.						RSbest %	Distance to nearest sonde station & Comments
		Time UTC	Lat	Long	RS No	WMO No.	Name	Time	Lat	Long		
7	10/01/2004	23:17	68.2N	31.4W	1	04360	Tasiilaq	23:20	65.59N	37.63W	50	400km. Warm/Occluded front to the east of Greenland.
					2	04339	Ittoqqortoormiit	23:00	70.48N	21.95W	50	
					3	04220	Aasiaat	23:29	68.69N	52.84W	0	
					4	04270	Narsarsuaq	23:00	61.15N	45.43W	0	
8	20/01/2004	11:13	44.5N	97.2W	1	72649	Chanhassen	11:07	44.84N	93.55W	70	290km.
					2	72558	Omaha	11:00	41.31N	96.36W	10	
					3	72662	Rapid City	11:36	44.08N	103.20W	10	
					4	72562	North Platte	11:01	41.13N	100.68W	10	
9	4/3/2004	12:32	13.9N	0.4W	1	65503	Ouagadougou	10:31	12.35N	1.51W	50	210km.
					2	61052	Niamey	11:55	13.48N	2.16E	50	
					3	61291	Bamako	10:32	12.53N	7.95W	0	
10	9/3/2004	00:54	12.7N	8.7W	1	61291	Bamako	10:32	12.53N	7.95W	90	90km.The satellite temperature profile is erroneous.
					2	61052	Niamey	11:55	13.48N	2.16E	10	
11	14/3/2004	23:42	52.8N	12.6E	1	10393	Lindenberg	22:48	52.2N	14.1E	50	120km. Frontal systems to the north and south.
					2	10184	Greifswald	22:45	54.1N	13.4E	30	
					3	10035	Schleswig	22:47	54.5N	9.6E	10	
					4	10200	Emden	23:45	52.4N	7.2E	10	
12	17/3/2004	00:49	66.0N	37.3W	1	04360	Tasiilaq	23:03	65.59N	37.63W	100	46km. Occluded front on the satellite profile.
					2	04270	Narsarsuaq	23:00	61.15N	45.43W	0	
					3	04220	Aasiaat	23:05	68.69N	52.84W	0	
					4	04339	Ittoqqortoormiit	23:01	70.48N	21.95W	0	
13	17/3/2004	12:42	14.2N	15.2W	1	61291	Bamako	10:31	12.53N	7.95W	34	810km.
					2	65503	Ouagadougou	10:31	12.35N	1.51W	33	
					3	61052	Niamey	?	13.48N	2.16E	33	

No.	Date UTC	Satellite			Radiosondes. In order of distance from satellite profile, RS1 nearest.						RSbest %	Distance to nearest sonde station & Comments
		Time UTC	Lat	Long	RS No	WMO No.	Name	Time	Lat	Long		
14	20/03/2004	12:55	13.5N	0.3E	1	61052	Niamey	?	13.48N	2.16E	0	200km. 61052 only Temp part D.
					2	65503	Ouagadougou	10:31	12.35N	1.51W	60	
					3	61291	Bamako	10:30	12.53N	7.95W	40	
15	21/3/2004	23:15	53.3N	8.7E	1	10200	Emden	23:45	52.4N	7.2E	50	120km. 10393 no winds.
					2	10035	Schleswig	22:52	54.5N	9.6E	50	
					3	10184	Greifswald	22:45	54.1N	13.4E	0	
					4	10393	Lindenberg	23:06	52.2N	14.1E	0	
16	22/3/2004	00:42	66.4N	48.6W	1	04220	Aasiaat	23:45	68.69N	52.84W	50	315km.
					2	04270	Narsarsuaq	23:00	61.15N	45.43W	25	
					3	04360	Tasiilaq	23:04	65.59N	37.63W	25	
					4	04339	Ittoqqortoormiit	23:02	70.48N	21.95W	0	
17	23/3/2004	23:01	14.0N	7.4W	1	61291	Bamako	22:31	12.53N	7.95W	70	175km.
					2	61641	Dakar	22:42	14.73N	17.50W	30	
18	26/3/2004	12:41	25.2S	151.0E	1							No radiosonde ascents available from the web site for this day.
					2							
					3							
					4							
19	27/3/2004	00:48	16.1N	10.5W	1	61291	Bamako	22:33	12.53N	7.95W	40	480km. 61641 & 61052 no TEMP part B
					2	61641	Dakar	?	14.73N	17.50W	40	
					3	61052	Niamey	?	13.48N	2.16E	20	
20	29/3/2004	12:05	13.0N	0.8W	1	65503	Ouagadougou	10:31	12.35N	1.51W	40	105km. 61052 No TEMP part B
					2	61052	Niamey	?	13.48N	2.16E	40	
					3	61291	Bamako	10:33	12.53N	7.95W	20	
21	2/4/2004	12:12	26.0S	148.8E	1	94510	Charleville	11:15	26.41S	146.26E	50	260km.


No.	Date UTC	Satellite			Radiosondes. In order of distance from satellite profile, RS1 nearest.						RSbest %	Distance to nearest sonde station & Comments
		Time UTC	Lat	Long	RS No	WMO No.	Name	Time	Lat	Long		
					2	94578	Brisbane	11:21	27.38S	153.13E	25	
					3	95527	Moree	11:15	29.48S	149.83E	25	
22	3/4/2004	00:18	17.1N	12.6W	1	61291	Bamako	23:31	12.53N	7.95W	80	710km. 61052 No TEMP part B
					2	61052	Niamey	?	13.48N	2.16E	20	
23	7/4/2004	11:14	13.4N	1.9W	1	61052	Niamey	?	13.48N	2.16E	70	440km. 61052 No TEMP part B
					2	61291	Bamako	10:33	12.53N	7.95W	30	
					3							
24	9/4/2004	11:41	25.9S	147.2E	1	94510	Charleville	11:15	26.41S	146.26E	50	110km.
					2	94578	Brisbane	11:16	27.38S	153.13E	25	
					3	95527	Moree	11:15	29.48S	149.83E	25	
25	12/4/2004	11:56	27.3S	149.6E	1	95527	Moree	11:15	29.48S	149.83E	34	240km.
					2	94510	Charleville	11:15	26.41S	146.26E	33	
					3	94578	Brisbane	11:16	27.38S	153.13E	33	
26	19/4/04	12:38	37.2N	139.0E	1	47646	Tateno	11:34	36.05N	140.13E	30	165km.
					2	47600	Wajima	11:30	37.38N	136.90E	30	
					3	47590	Sendai	11:30	38.26N	140.90E	20	
					4	47582	Akita	11:30	39.71N	140.10E	20	
27	26/4/04	12:06	37.4N	137.7E	1	47600	Wajima	11:30	37.38N	136.90E	100	70km.
					2	47646	Tateno	11:30	36.05N	140.13E	0	
					3	47590	Sendai	11:30	38.26N	140.90E	0	
					4	47582	Akita	11:30	39.71N	140.10E	0	
28	5/5/2004	23:24	66.1N	49.6W	1	04220	Aasiaat	22:59	68.69N	52.84W	40	320km.Warm front to the south

No.	Date UTC	Satellite			Radiosondes. In order of distance from satellite profile, RS1 nearest.						RSbest %	Distance to nearest sonde station & Comments
		Time UTC	Lat	Long	RS No	WMO No.	Name	Time	Lat	Long		
					2	04360	Tasiilaq	22:59	65.59N	37.63W	30	of Greenland.
					3	04270	Narsarsuaq	23:00	61.15N	45.43W	30	
					4	04339	Ittoqqortoormiit	23:01	70.48N	21.95W	0	
29	07/06/2004	11:17	44.2N	95.7W	1	72649	Chanhassen	11:16	44.84N	93.55W	40	185km.
					2	72558	Omaha	11:16	41.31N	96.36W	20	
					3	72562	North Platte	11:11	41.13N	100.68W	20	
					4	72662	Rapid City	11:05	44.08N	103.20W	20	
30	27/6/2004	12:12	54.2N	9.6E	1	10035	Schleswig	10:49	54.53N	9.55E	80	40km. Warm and cold front to the west and an upper air cold front to the east of the satellite profile.
					2	10200	Emden	10:45	53.38N	7.23E	10	
					3	10184	Greifswald	10:46	54.10N	13.40E	10	
					4	10393	Lindenberg	10:45	52.21N	14.11E	0	
31	31/07/2004	12:54	68.1N	36.3W	1	04360	Tasiilaq	11:11	65.59N	37.63W	70	300km.
					2	04339	Ittoqqortoormiit	10:59	70.48N	21.95W	10	
					3	04220	Aasiaat	10:59	68.69N	52.84W	10	
					4	04270	Narsarsuaq	11:00	61.15N	45.43W	10	
32	02/08/2004	12:16	63.1N	157.3W	1	70231	McGrath	11:03	62.96N	155.61W	70	90km
					2	70219	Bethel	11:02	60.78N	161.80W	10	
					3	70200	Nome	11:01	64.50N	165.43W	10	
					4	70133	Kotzebue	11:02	66.86N	162.63W	10	
33	09/08/2004	00:37	15.4N	11.2W	1	61291	Bamako	22:32	12.53N	7.95W	50	470km. 61291 Only Parts A&D 61052 No Part B
					2	61641	Dakar	?	14.73N	17.50W	50	
					3	61052	Niamey	?	13.48N	2.16E	0	
34	17/08/2004	00:16	25.5S	48.9W	1	83840	Curitiba	23:29	25.51S	49.16W	100	26km.

No.	Date UTC	Satellite			Radiosondes.						RSbest %	Distance to nearest sonde station & Comments
		Time UTC	Lat	Long	In order of distance from satellite profile, RS1 nearest.							
					RS No	WMO No.	Name	Time	Lat	Long		
					2	83971	Porto Alegre	23:30	30.00S	51.18W	0	
					3	83746	Galeao	23:30	22.81S	43.25W	0	
35	20/8/2004	23:36	14.6N	12.5W	1	61641	Dakar	?	14.73N	17.50W	50	540km. 61641 only Temp part A. 61291 & 61052 no TEMP part B.
					2	61291	Bamako	22:36	12.53N	7.95W	50	
					3	61052	Niamey	?	13.48N	2.16E	0	
36	1/09/2004	11:38	28.4S	149.3E	1	95527	Moree	11:15	29.48S	149.83E	80	130km.
					2	94578	Brisbane	11:16	27.38S	153.13E	10	
					3	94510	Charleville	11:15	26.41S	146.26E	10	
37	10/09/2004	12:32	67.1N	34.6W	1	04360	Tasiilaq	11:04	65.59N	37.63W	70	215km. Occluded front in area.
					2	04339	Ittoqqortoormiit	11:03	70.48N	21.95W	10	
					3	04220	Aasiaat	10:59	68.69N	52.84W	10	
					4	04270	Narsarsuaq	11:00	61.15N	45.43W	10	
38	14/09/2004	00:35	18.2N	65.8W	1	78526	San Juan	23:12	18.45N	66.00W	100	35km. 78970 (RS3) Temp data hidden between 13 and 22.4km.
					2	78954	Grantley Adams	23:01	13.06N	59.48W	0	
					3	78970	Piarco	23:48	10.61N	61.35W	0	
39	15/09/2004	12:13	68.4N	35.8W	1	04360	Tasiilaq	11:05	65.59N	37.63W	70	325km.
					2	04339	Ittoqqortoormiit	11:01	70.48N	21.95W	10	
					3	04220	Aasiaat	10:59	68.69N	52.84W	10	
					4	04270	Narsarsuaq	11:00	61.15N	45.43W	10	
40	30/11/2004	23:48	66.0N	35.1W	1	04360	Tasiilaq	23:31	65.59N	37.63W	80	125km04220 (RS4) No Temp

No.	Date UTC	Satellite			Radiosondes. In order of distance from satellite profile, RS1 nearest.						RSbest %	Distance to nearest sonde station & Comments
		Time UTC	Lat	Long	RS No	WMO No.	Name	Time	Lat	Long		
					2	04339	Ittoqqortoormiit	23:14	70.48N	21.95W	20	part B. Weather front N-S along the middle of the area.
					3	04270	Narsarsuaq	23:00	61.15N	45.43W	0	
					4	04220	Aasiaat	?	68.69N	52.84W	0	
41	8/12/2004	12:30	68.8N	27.4W	1	04339	Ittoqqortoormiit	11:04	70.48N	21.95W	100	285km. Weather front N-S.
					2	04360	Tasiilaq	11:12	65.59N	37.63W	0	
					3	04220	Aasiaat	10:59	68.69N	52.84W	0	
					4	04270	Narsarsuaq	11:02	61.15N	45.43W	0	
42	11/12/2004	00:25	65.7N	13.1E	1	01152	Bodo	23:10	67.3N	14.4E	50	180km SW. Warm front N-S across area.
					2	01241	Orland	23:08	63.7N	9.6E	50	
					3	02365	Sundsvall	23:30	62.5N	17.5E	0	
					4	02185	Lulea-Kallax	23:30	65.6N	22.1E	0	
43	16/12/2004	12:19	36.5N	140.0E	1	47646	Tateno	11:34	36.05N	140.13E	60	50km.
					2	47590	Sendai	11:30	38.26N	140.90E	20	
					3	47600	Wajima	11:30	37.38N	136.90E	20	
					4	47582	Akita	11:30	39.71N	140.10E	0	
44	20/12/2004	12:18	15.9N	8.7W	1	61291	Bamako	12:37	12.53N	7.95W	50	380km.
					2	65503	Ouagadougou	10:31	12.35N	1.51W	20	
					3	61641	Dakar	10:41	14.73N	17.50W	20	
					4	61052	Niamey	10:33	13.48N	2.16E	10	
45	22/12/2004	12:21	37.4N	138.4E	1	47600	Wajima	11:30	37.38N	136.90E	80	130km.

No.	Date UTC	Satellite			Radiosondes. In order of distance from satellite profile, RS1 nearest.						RSbest %	Distance to nearest sonde station & Comments
		Time UTC	Lat	Long	RS No	WMO No.	Name	Time	Lat	Long		
					2	47646	Tateno	11:30	36.05N	140.13E	10	
					3	47590	Sendai	11:30	38.26N	140.90E	10	
					4	47582	Akita	12:30	39.71N	140.10E	0	
46	24/12/2004	11:31	63.8N	9.8E	1	01241	Orland	23:08	63.7N	9.6E	100	15km.
					2	02365	Sundsvall	23:30	62.5N	17.5E	0	
					3	01152	Bodo	23:10	67.3N	14.4E	0	
					4	02185	Lulea-Kallax	23:30	65.6N	22.1E	0	
47	26/12/2004	00:54	24.8S	49.1W	1	83840	Curitiba	23:30	25.51S	49.16W	100	70km.
					2	83827	Foz Do Iguacu	23:31	25.51S	54.58W	0	
					3	83971	Porto Alegre	23:32	30.00S	51.18W	0	
48	29/12/2004	11:03	69.3N	28.2W	1	04339	Ittoqqortoormiit	11:00	70.48N	21.95W	75	275km.
					2	04360	Tasiilaq	11:13	65.59N	37.63W	25	
					3	04220	Aasiaat	11:02	68.69N	52.84W	0	
					4	04270	Narsarsuaq	11:00	61.15N	45.43W	0	

Ref: SAF/GRAS/DMI/REP/VS8/001 Issue: Version 1.0 Date: 23 May 2008 Document: VS8-report_18-04-08_v10.doc	GRAS Meteorology SAF Document	<i>EUMETSAT</i> DMI ECMWF IEEC Met Office	 www.grassaf.org
---	----------------------------------	---	---

This Page is left intentionally blank.

Annex B

Table 3 Radiosonde equipment

WMO No.	Country	Name	Sonde	System	Solar and infrared radiation correction	Tracking system
01152	NORWAY	Bodo	RS80/AU/L	Vaisala Digicora I, II or Marwin	Solar and infrared corrected automatically by radiosonde system	LORAN-C
01241	NORWAY	Orland III	RS80/AU/L	Vaisala Digicora I, II or Marwin	Solar and infrared corrected automatically by radiosonde system	LORAN-C
02185	SWEDEN	Lulea-Kallax	RS80/AU/L	Vaisala Digicora I, II or Marwin	Solar and infrared corrected automatically by radiosonde system	LORAN-C
02365	SWEDEN	Sundsvall	RS80/AU/L	Vaisala Digicora I, II or Marwin	Solar and infrared corrected automatically by radiosonde system	LORAN-C
10035	GERMANY	Schleswig	RS80/R	Vaisala PCCora	Solar and infrared corrected automatically by radiosonde system	Automatic with auxiliary ranging
10184	GERMANY	Greifswald	RS80/R	Vaisala PCCora	Solar and infrared corrected automatically by radiosonde system	Automatic with auxiliary ranging
10200	GERMANY	Emden	RS80/R	Vaisala PCCora	Solar and infrared corrected automatically by radiosonde system	Automatic with auxiliary ranging
10393	GERMANY	Lindenberg	RS80/R	Vaisala PCCora	Solar and infrared corrected automatically by radiosonde system	Automatic with auxiliary ranging
96413	MALAYSIA	Kuching	RS80/G	Vaisala Digicora I, II or Marwin	Solar and infrared corrected automatically by radiosonde system	Automatic satellite navigation
96441	MALAYSIA	Bintulu	RS80/G	Vaisala Digicora I, II or Marwin	Solar and infrared corrected automatically by radiosonde system	Automatic satellite navigation
96471	MALAYSIA	Kota Kinabalu	RS80/G	Vaisala Digicora I, II or Marwin	Solar and infrared corrected automatically by radiosonde system	Automatic satellite navigation
96481	MALAYSIA	Tawau	RS80/G	Vaisala Digicora I, II or Marwin	Solar and infrared corrected automatically by radiosonde system	Automatic satellite navigation
04220	GREENLAND	Aasiaat	RS90	Vaisala Digicora I, II or Marwin	Solar and infrared corrected automatically by radiosonde system	Automatic satellite navigation
04270	GREENLAND	Narsarsuaq	RS90	Vaisala Digicora I, II or Marwin	Solar and infrared corrected automatically by radiosonde system	Automatic satellite navigation
04339	GREENLAND	Ittoqqortoormiit	RS90	Vaisala Digicora I, II or Marwin	Solar and infrared corrected automatically by radiosonde system	Automatic cross chain Loran-C
04360	GREENLAND	Tasiilaq	RS90	Vaisala Digicora I, II or Marwin	Solar and infrared corrected automatically by radiosonde system	Automatic cross chain Loran-C
78526	PUERTO RICO	San Juan	VIZ-B2		No correction	Automatic with auxiliary optical direction finding
78954	BARBADOS	Grantley Adams	VIZ-B2		No correction	Automatic with auxiliary optical direction finding
78970	TRINIDAD	Piarco	VIZ-B2		No correction	Automatic with auxiliary optical direction finding
72649	USA	Chanhassen	RS80-57H		Solar and infrared corrected automatically by radiosonde system	Automatic with auxiliary radio direction finding
72558	USA	Omaha	RS80-57H		Solar and infrared corrected automatically by radiosonde system	Automatic with auxiliary radio direction finding

WMO No.	Country	Name	Sonde	System	Solar and infrared radiation correction	Tracking system
72662	USA	Rapid City	RS80-57H		Solar and infrared corrected automatically by radiosonde system	Automatic with auxiliary radio direction finding
72562	USA	North Platte	RS80-57H		Solar and infrared corrected automatically by radiosonde system	Automatic with auxiliary radio direction finding
65503	BURKINO FASO	Ouagadougou	RS80	Star	Solar and infrared corrected automatically by radiosonde system	Automatic satellite navigation
61052	NIGER	Niamey	RS80	Vaisala Digicora I, II or Marwin	Solar and infrared corrected automatically by radiosonde system	Automatic satellite navigation
61291	MALI	Bamako	RS80	Star	Solar and infrared corrected automatically by radiosonde system	Automatic satellite navigation
61641	SENEGAL	Dakar	RS80	Vaisala Digicora I, II or Marwin	Solar and infrared corrected automatically by radiosonde system	Automatic satellite navigation
94866	AUSTRALIA	Melbourne	RS80/R	Vaisala PC-Cora	Solar and infrared corrected automatically by radiosonde system	
94910	AUSTRALIA	Wagga Wagga	RS80/R	Vaisala PC-Cora	Solar and infrared corrected automatically by radiosonde system	
94672	AUSTRALIA	Adelaide	RS80/R	Vaisala PC-Cora	Solar and infrared corrected automatically by radiosonde system	
94711	AUSTRALIA	Cobar	RS80/AU/G	Vaisala Digicora2	Solar and infrared corrected automatically by radiosonde system	
94374	AUSTRALIA	Rockhampton	RS80/R	Vaisala PC-Cora	Solar and infrared corrected automatically by radiosonde system	
94510	AUSTRALIA	Charleville	RS80/AU/G	Vaisala Digicora2	Solar and infrared corrected automatically by radiosonde system	Automatic satellite navigation
94578	AUSTRALIA	Brisbane	RS80/R	Vaisala PC-Cora	Solar and infrared corrected automatically by radiosonde system	Automatic with auxiliary ranging
95527	AUSTRALIA	Moree	RS80/AU/G	Vaisala Digicora2	Solar and infrared corrected automatically by radiosonde system	Automatic satellite navigation
70231	USA	McGrath	RS80-57H		Solar and infrared corrected automatically by radiosonde system	Automatic with auxiliary radio direction finding
70219	USA	Bethel	RS80-57H		Solar and infrared corrected automatically by radiosonde system	Automatic with auxiliary radio direction finding
70200	USA	Nome	RS80-57H		Solar and infrared corrected automatically by radiosonde system	Automatic with auxiliary radio direction finding
70133	USA	Kotzebue	RS80-57H		Solar and infrared corrected automatically by radiosonde system	Automatic with auxiliary radio direction finding
83840	BRAZIL	Curitiba	VIS Mk II	W9000	No correction	Automatic with auxiliary radio direction finding
83971	BRAZIL	Porto Alegre	VIS Mk II	W9000	No correction	Automatic with auxiliary radio direction finding
83746	BRAZIL	Galeao	VIS Mk II	W9000	Solar corrected automatically by radiosonde system	Automatic with auxiliary radio direction finding
83827	BRAZIL	Foz Do Iguacu	VIS Mk II	W9000	Solar corrected automatically by radiosonde system or no correction	Automatic with auxiliary radio direction finding

Annex C

Table 4 RSK datasets for Satellite and Radiosondes

Radiosonde dataset								
Column 1	Column 2	Column 3	Column 4	Column 5	Column 6	Column 7	Column 8	Column 9
Pressure hPa	Height (m)	Temperature (deg C)	Temperature (deg K)	Dew Point	Humidity (%)	Mixing ratio g/Kg	Wind direction (degs)	Wind Speed (Knots)
			Converted from temperature (deg C) +273.15					
Satellite dataset								
Column 1	Column 2	Column 3	Column 4	Column 5	Column 6	Column 7	Column 8	
Pressure hPa	Derived Temperature (K)	Model Temperature (K)	Geopotential Height (km)	Geopotential Height (m)	Humidity (g/kg)	Model Humidity (g/Kg)	Mixing ratio (g/kg)	
		ECMWF profile temperature		Converted from the height in km.		ECMWF profile humidity	A copy of Humidity (g/Kg)	
RSbest dataset								
Column 1	Column 2	Column 3						
Height (m)	Temperature Interpolated best fit profile. (deg K)	Mixing ratio Interpolated best fit profile. g/Kg						
RSbest+ dataset								
Column 1	Column 2	Column 3	Column 4					
Height (m)	Temperature Interpolated best fit profile. (deg K)	Mixing ratio Interpolated best fit profile. g/Kg	Temperature Interpolated best fit profile. (deg K) Called Model Temperature (deg K)					

Annex D

Maps of Comparison locations.

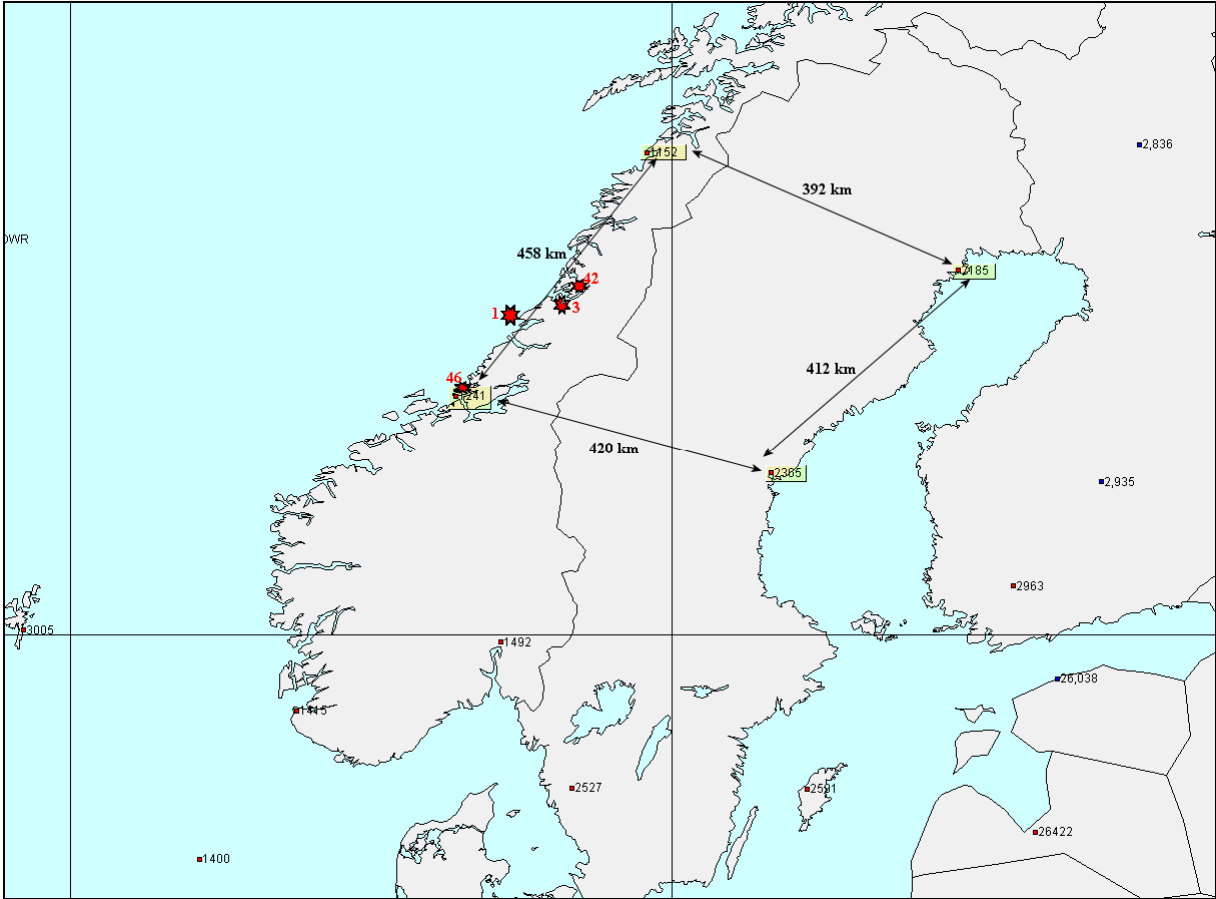


Figure D1 Location of Radiosonde stations and Satellite profiles in Scandinavia

Figure D1 above, shows the location and distance between the radiosonde stations in Scandinavia. The approximate location of the satellite profiles is indicated by the red star, and the number beside this indicates which comparison it was for.

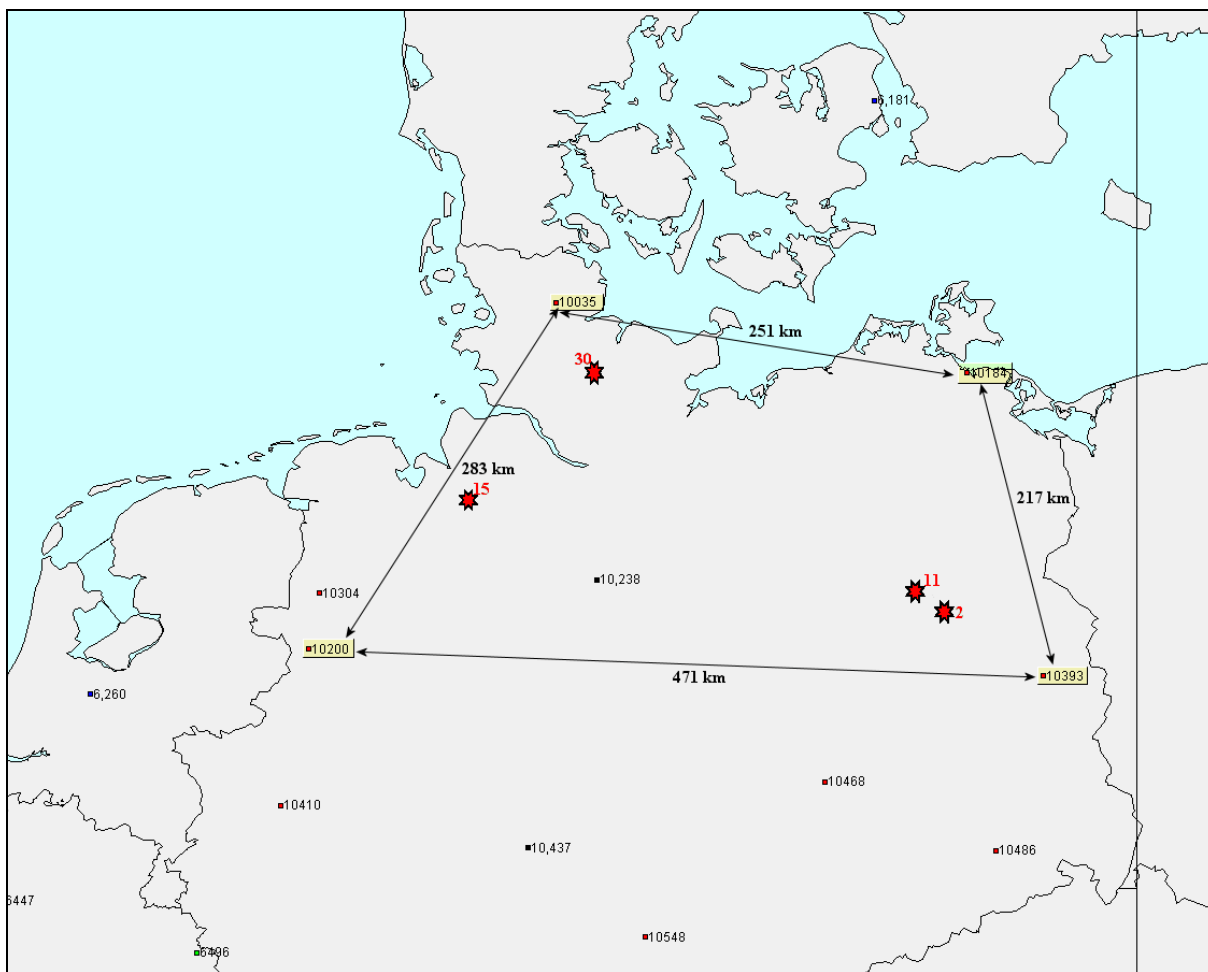


Figure D2 Location of Radiosonde stations and satellite profile in Germany.

Figure D2 above, shows the location and distance between the radiosonde stations in Northern Germany. The approximate location of the satellite profiles is indicated by the red star, and the number beside this indicates which comparison it was for.

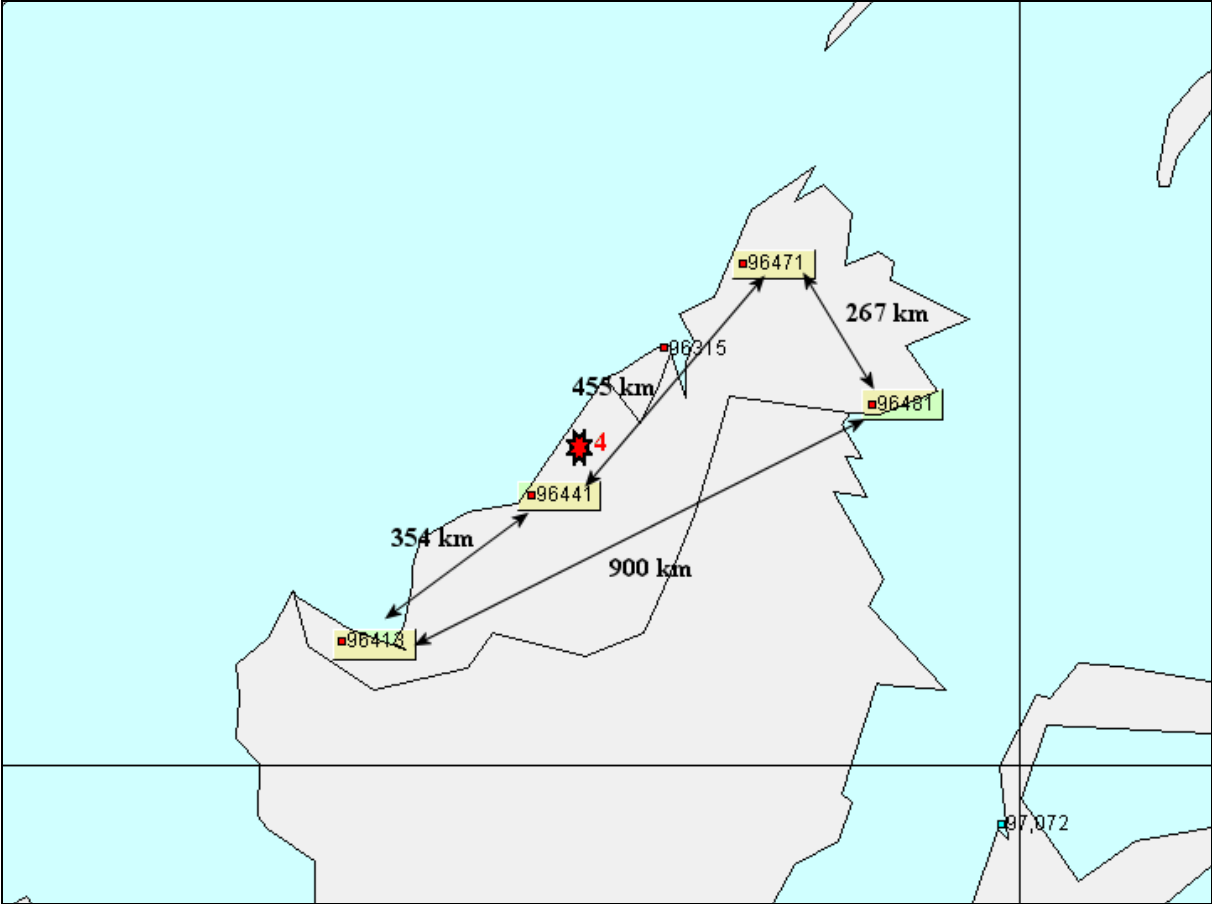


Figure D3 Location of Radiosonde stations and satellite profile in Sarawak and Sabah, Malaysia

Figure D3 above, shows the location and distance between the radiosonde stations in Malaysia. The approximate location of the satellite profiles is indicated by the red star, and the number beside this indicates which comparison it was for.

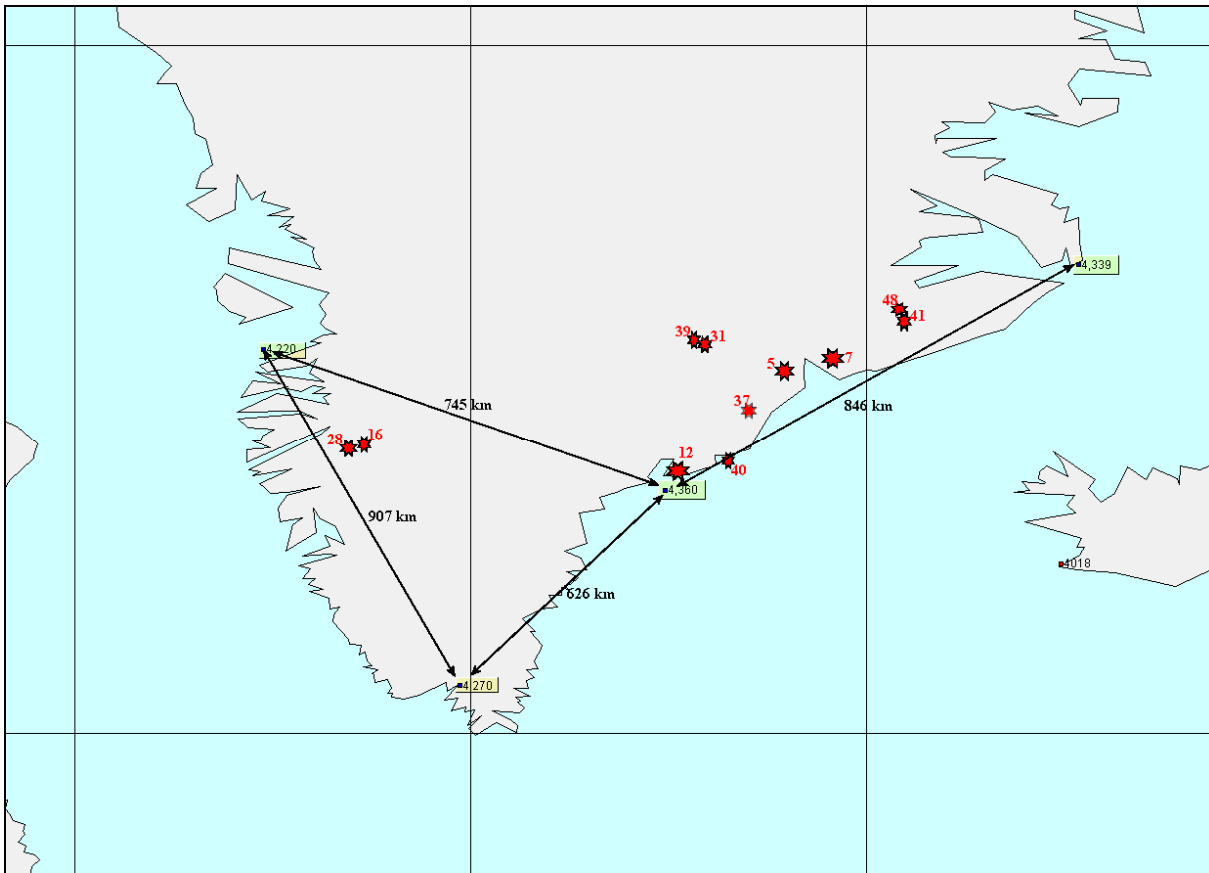


Figure D4 Location of Radiosonde stations and satellite profile in Greenland.

Figure D4 above, shows the location and distance between the radiosonde stations in Greenland. The approximate location of the satellite profiles is indicated by the red star, and the number beside this indicates which comparison it was for.

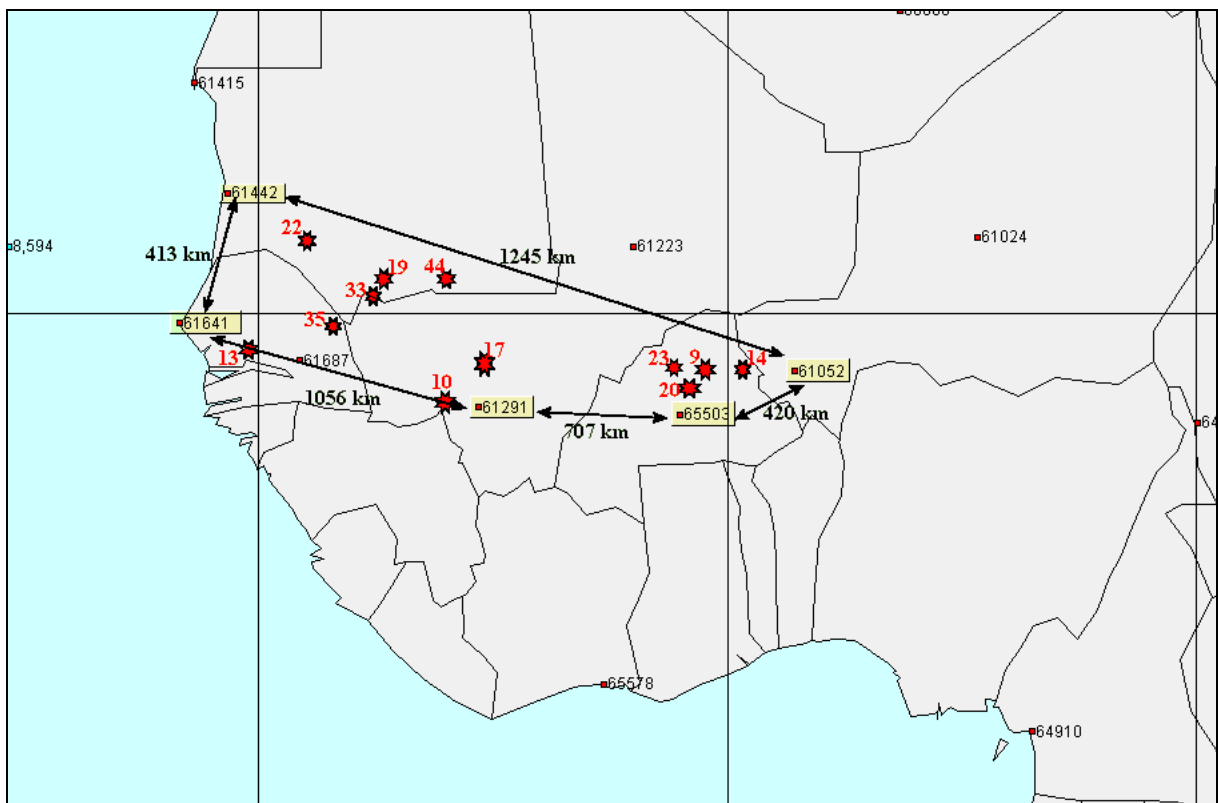


Figure D5 Location of Radiosonde stations and satellite profile in West Africa.

Figure D5 above, shows the location and distance between the radiosonde stations in West Africa. The approximate location of the satellite profiles is indicated by the red star, and the number beside this indicates which comparison it was for.

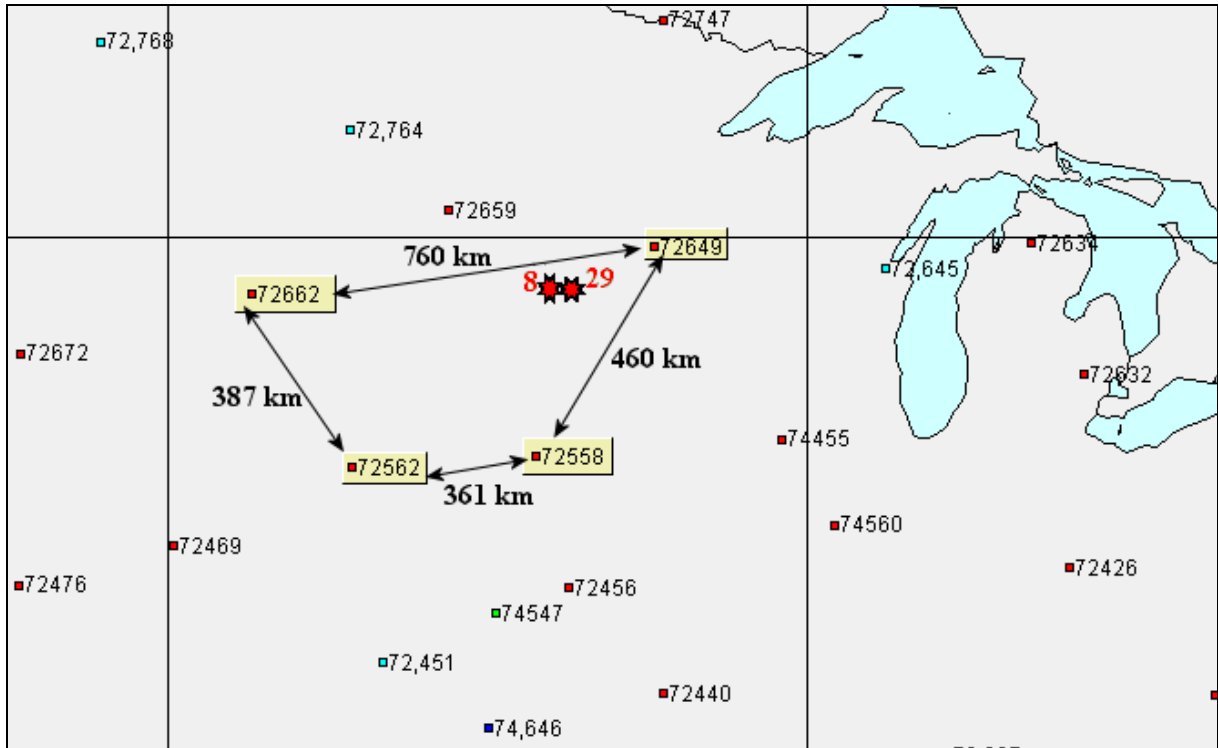


Figure D6 Location of Radiosonde stations and satellite profile in USA.

Figure D6 above, shows the location and distance between the radiosonde stations in the USA. The approximate location of the satellite profiles is indicated by the red star, and the number beside this indicates which comparison it was for.

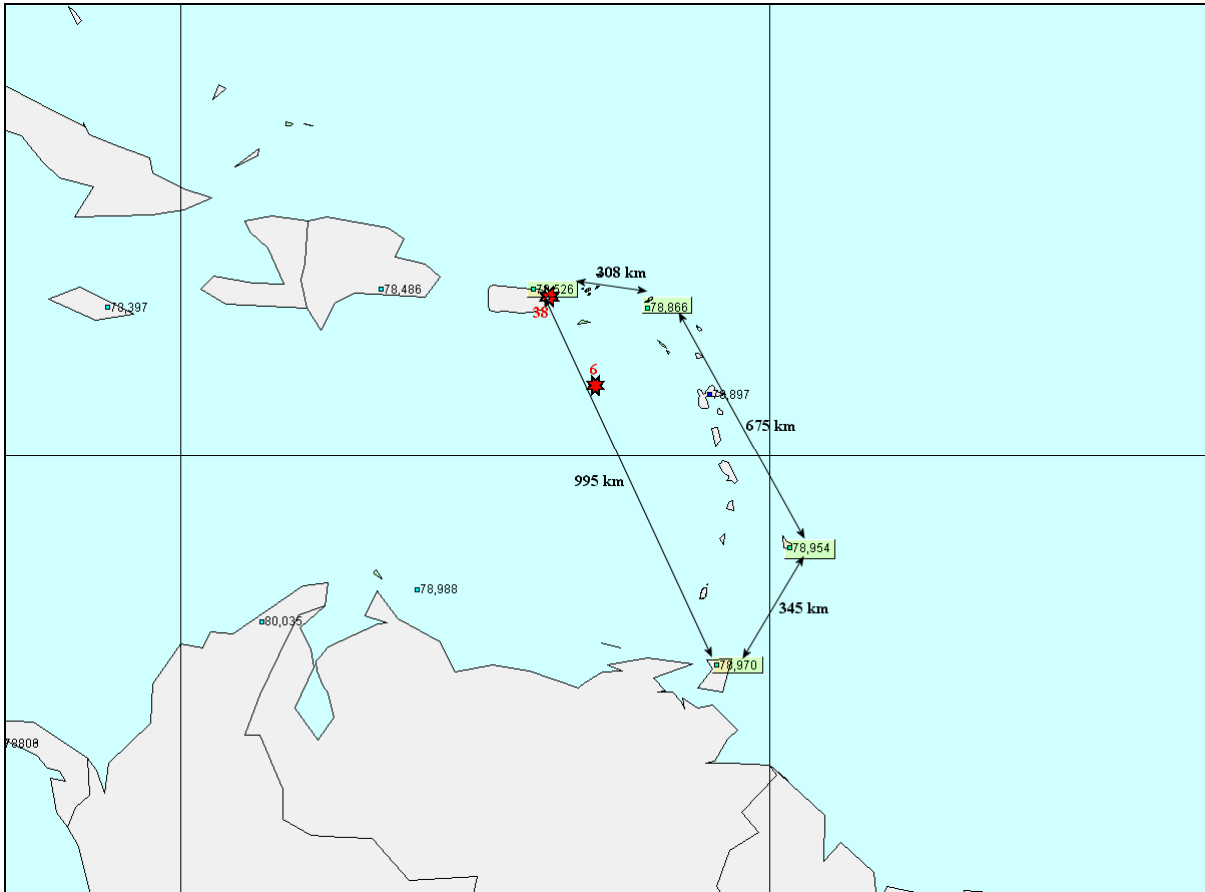


Figure D7 Location of Radiosonde stations and satellite profile in the Caribbean.

Figure D7 above, shows the location and distance between the radiosonde stations in the Caribbean. The approximate location of the satellite profiles is indicated by the red star, and the number beside this indicates which comparison it was for.

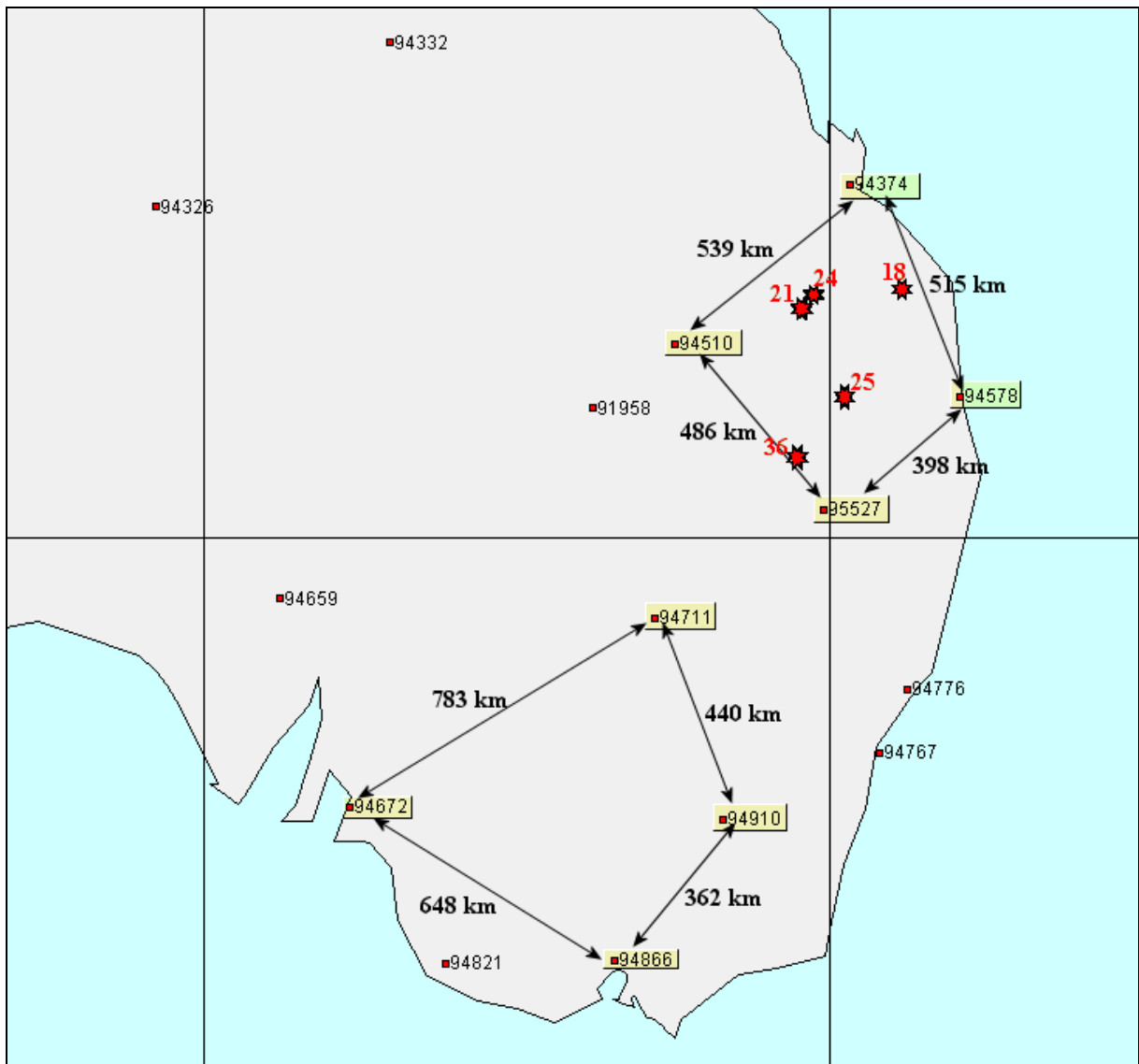


Figure D8 Location of Radiosonde stations and satellite profile in Australia.

Figure D8 above, shows the location and distance between the radiosonde stations in Australia. The approximate location of the satellite profiles is indicated by the red star, and the number beside this indicates which comparison it was for.

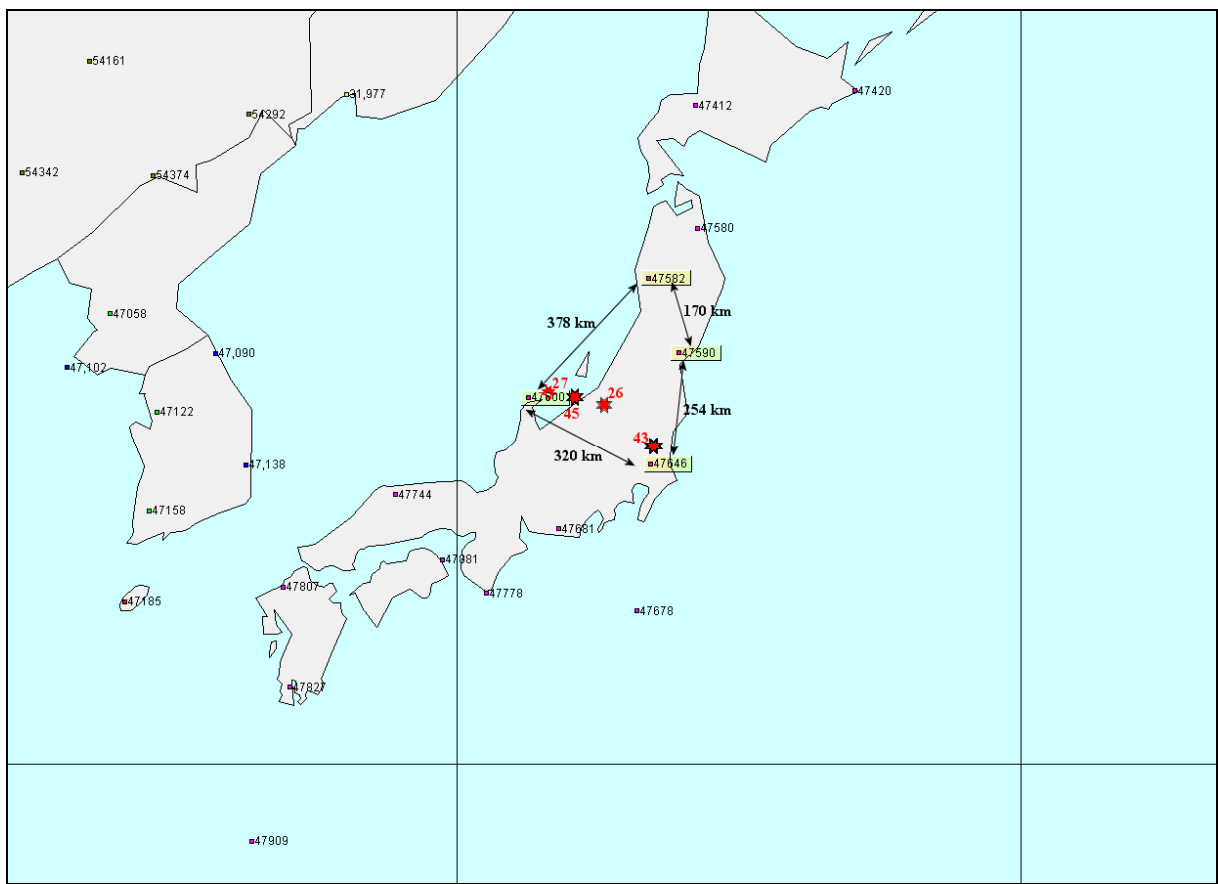


Figure D9 Location of Radiosonde stations and satellite profiles in Japan.

Figure D9 above, shows the location and distance between the radiosonde stations in Japan. The approximate location of the satellite profiles is indicated by the red star, and the number beside this indicates which comparison it was for.

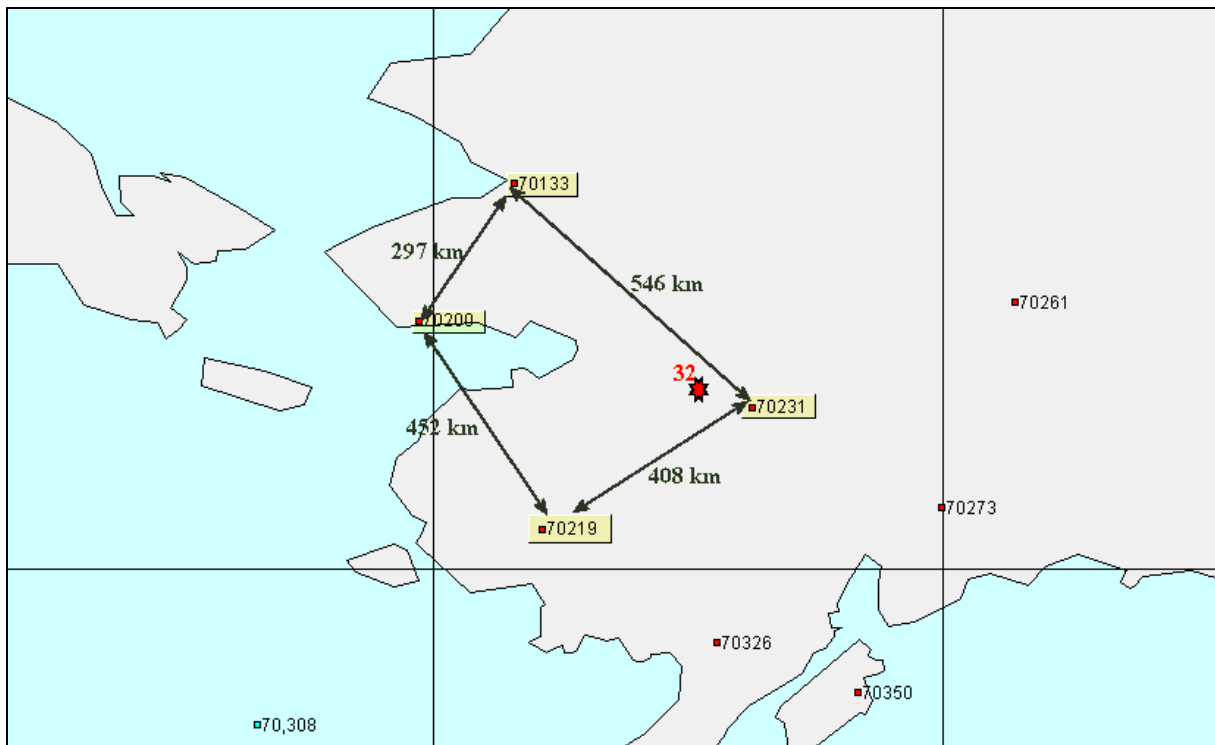


Figure D10 Location of Radiosonde stations and satellite profiles in Alaska.

Figure D10 above, shows the location and distance between the radiosonde stations in Alaska. The approximate location of the satellite profiles is indicated by the red star, and the number beside this indicates which comparison it was for.

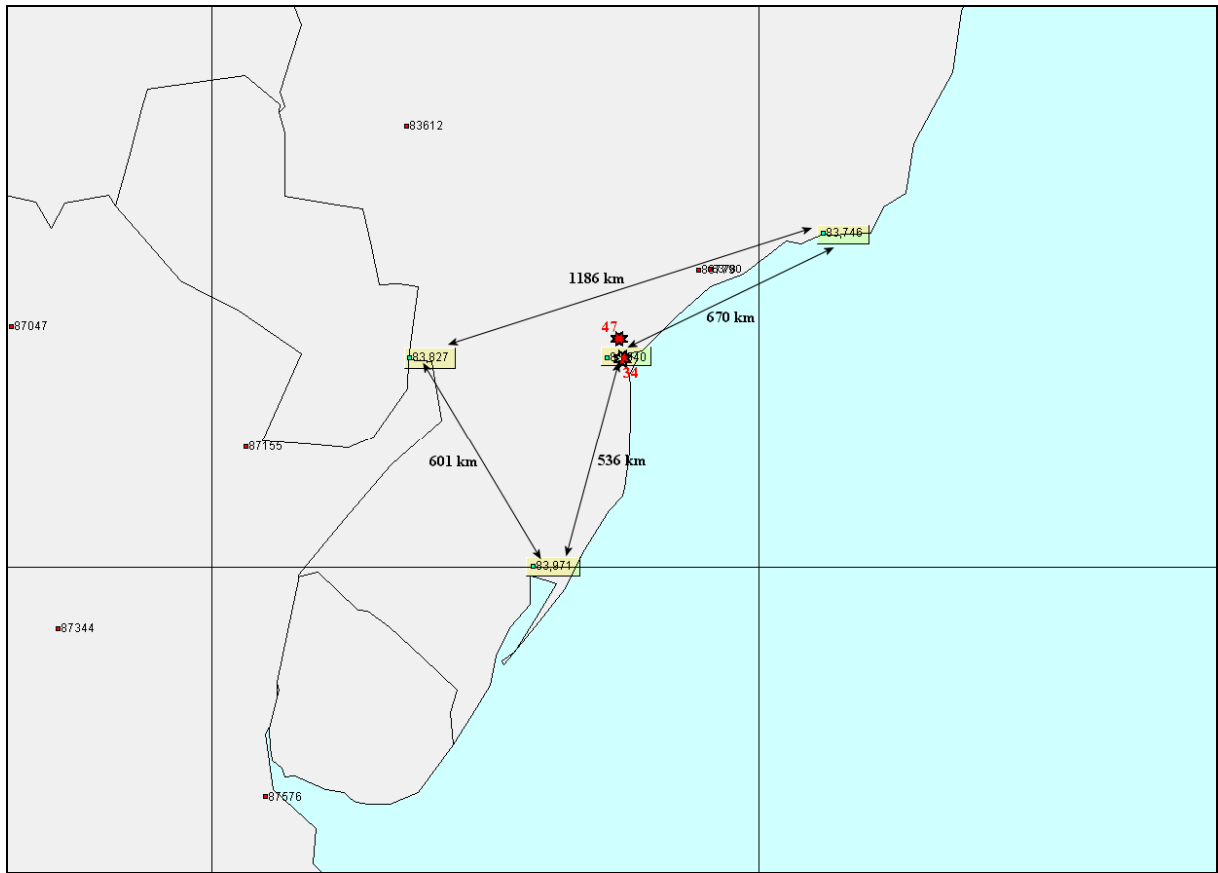


Figure D11 Location of Radiosonde stations and satellite profiles in Brazil.

Figure D11 above, shows the location and distance between the radiosonde stations in Brazil. The approximate location of the satellite profiles is indicated by the red star, and the number beside this indicates which comparison it was for.

Annex E

Explanation why comparisons 10, 16, 18 and 44 were excluded.



Figure E1 Comparison 10's erroneous satellite profile

Figure E1 above shows comparison 10 has an erroneous satellite profile so has been excluded from the dataset.

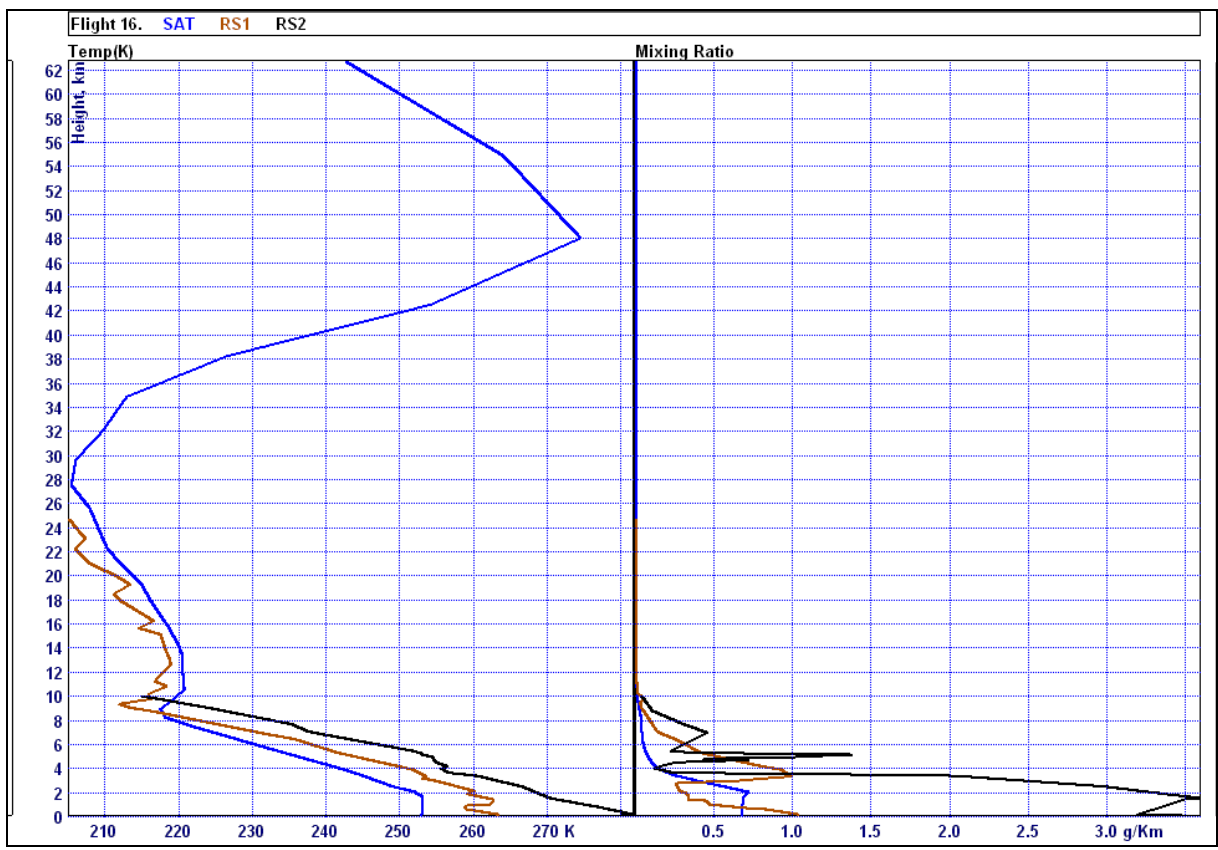


Figure E2 Comparison 16 satellite and radiosonde profiles.

Figure E2 above shows the satellite profile for comparison 16, this does not match any of the radiosonde profiles, therefore has been excluded from the dataset. The satellite profile for comparison 28 (see figure E3 below), which is in a comparable location to comparison 16, is similar to the radiosondes and is used in the statistics.



Figure E3 comparison 28

Comparison 18 has been excluded from the dataset as no radiosonde ascents could be retrieved for the area.



Figure E4 comparison 44 satellite and radiosonde profiles

Figure E4 above shows the satellite profile for comparison 44. This does not match the radiosonde profile in the lower troposphere, or just below the tropopause, therefore has been excluded from the dataset. The satellite profile for comparison 19 (see figure E5 below), which is in a comparable location to comparison 44, is similar to the radiosonde profiles therefore, is used in the statistics.



Figure E5 comparison 19

